



Day 3

# **Bridging Sequence, Structure and Interactions** **Environment, Evolution, Druggability,**

**Ivet Bahar**

Department of <sup>1</sup>Computational and Systems Biology  
School of Medicine, University of Pittsburgh, Pittsburgh, PA 15260

# Summary

## 1. Theory

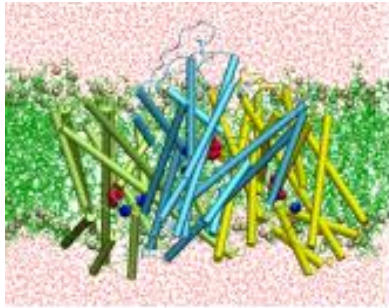
- a. Gaussian Network Model (GNM)
- b. Anisotropic Network Model (ANM)
- c. Resources/Servers/Databases (ProDy, DynOmics)

## 2. Bridging Sequence, Structure and Function

- a. Ensemble analysis using the ANM
- b. Combining sequence and structure analyses – signature dynamics
- c. Allosteric communication – sensors and effectors

## 3. Membrane proteins and druggability

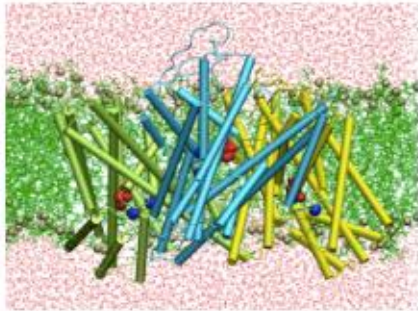
- a. Modeling environmental effects using elastic network models
- b. Modeling & simulations of Membrane Proteins with ENMs for lipids
- c. Druggability simulations



# membrANM

Membrane Anisotropic Network Model

# ANM for membrane proteins: membrANM



Membrane ANM (membrANM)

Learn how to include the effect of lipid bilayer in ENM study of membrane proteins dynamics.

[Go to Tutorial](#)

- Evaluating membrane proteins' dynamics in the presence of lipid bilayer
- Comparing global motions in the presence and absence of membrane
- Understanding mechanisms of protein-membrane remodeling

Implemented in ProDy and DynOmics

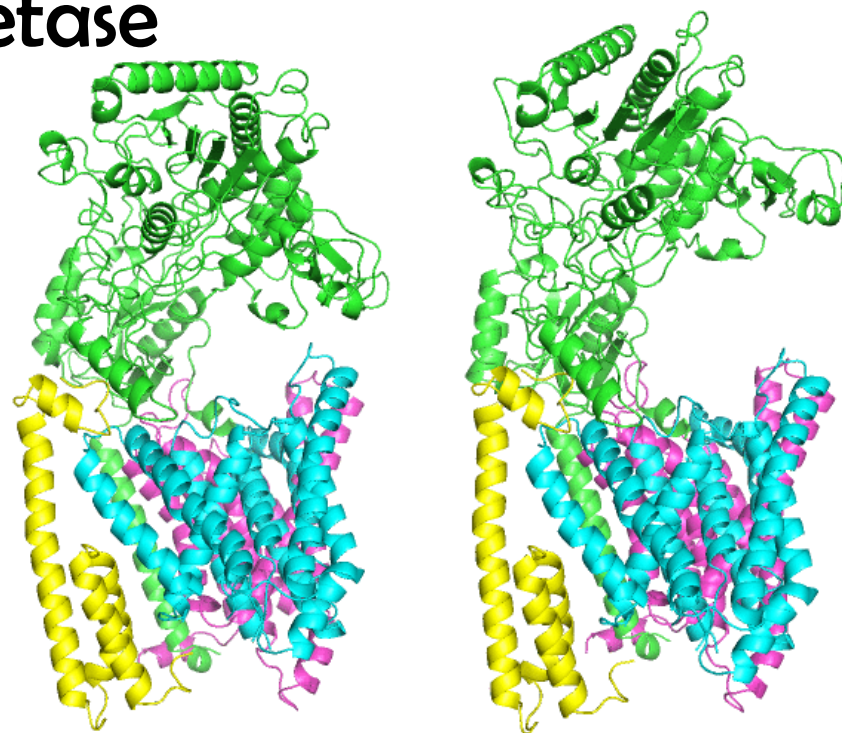
# MembrANM for $\gamma$ -secretase

The effect of the membrane environment can be incorporated in the ANM analysis by adopting

- envANM-membrANM or
- substructure-membrANM.

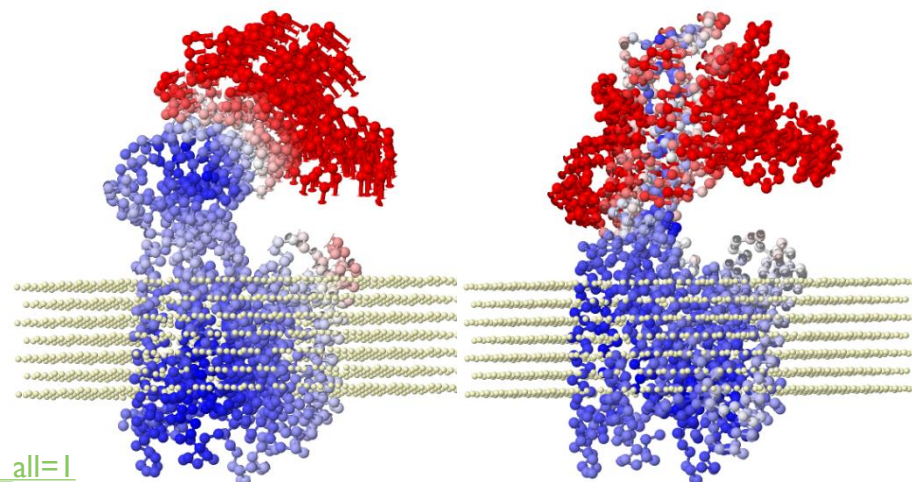
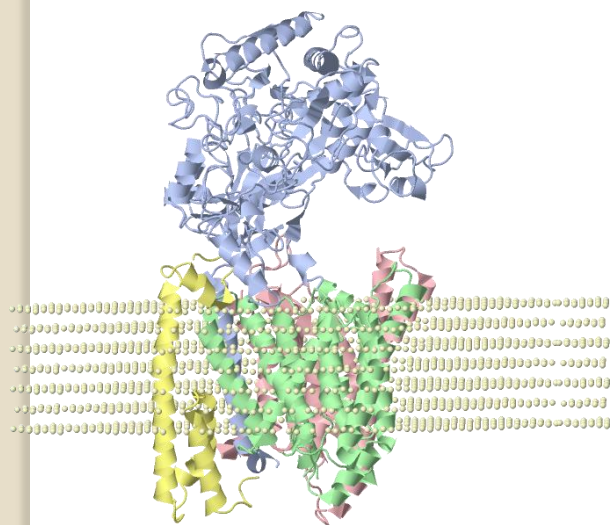
MembrANM results for the  $\gamma$ -secretase (PDB ID: 5FN2) can be viewed on the ENM server:

PyMol movies can be downloaded from DynOmics ENM server by generating “Full Atomic Structures for ANM-Driven Conformers”.



Mode 1 - bending

Mode 2 - twisting



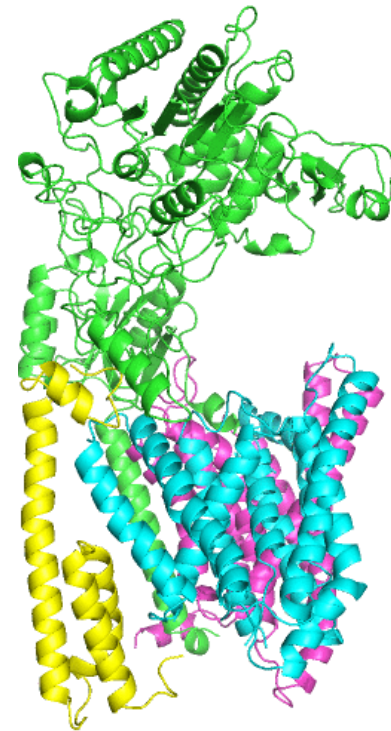
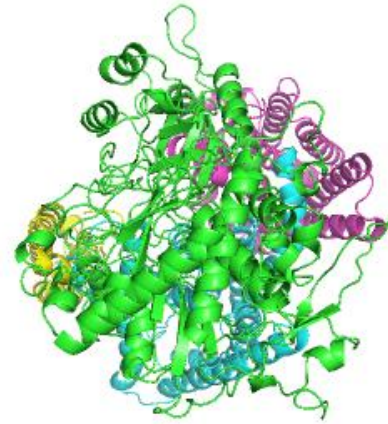
# MembrANM for $\gamma$ -secretase

The effect of the membrane environment can be incorporated in the ANM analysis by adopting

- envANM-membrANM or
- substructure-membrANM.

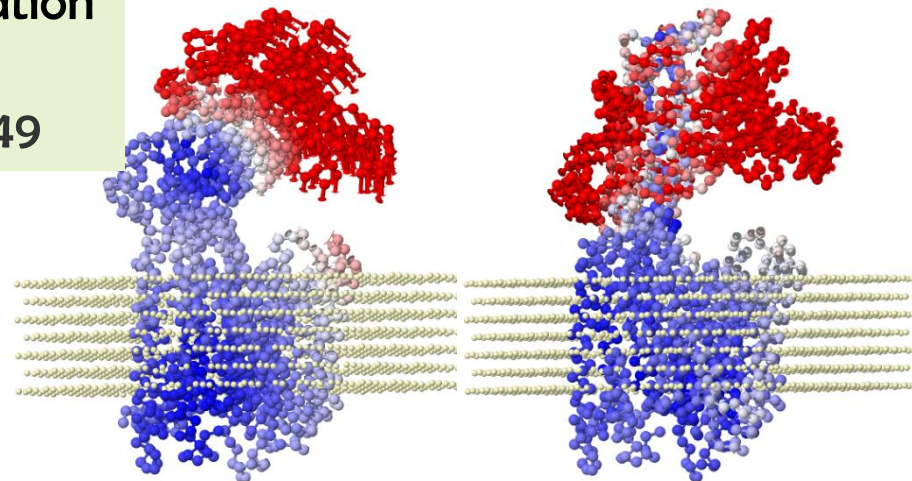
MembrANM results for the  $\gamma$ -secretase (PDB ID: 5FN2) can be viewed on the ENM server:

PyMol movies can be downloaded from DynOmics ENM server by generating “Full Atomic Structures for ANM-Driven Conformers”.



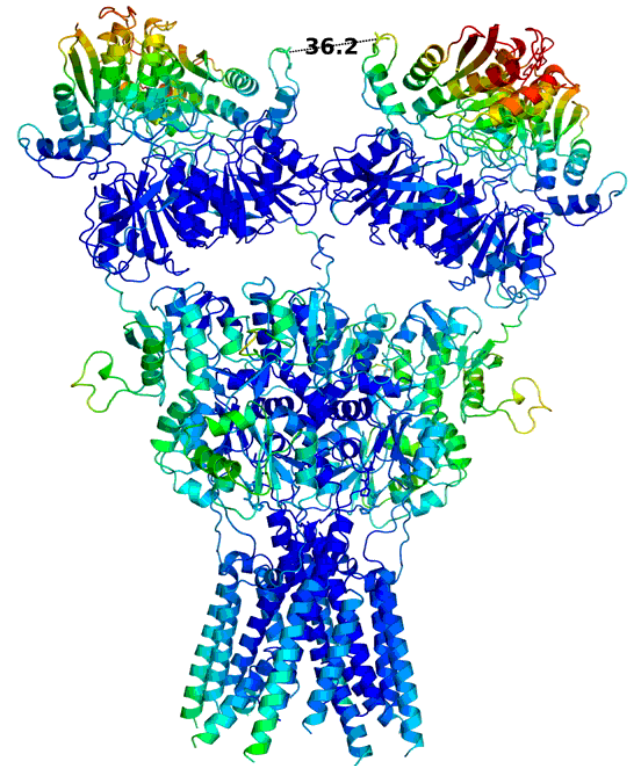
Mode 2 - twisting

Lee et al (2017) Allosteric Modulation of Intact  $\gamma$ -Secretase Structural Dynamics. *Biophys J* 113:2634-2649



# Collective dynamics of AMPA receptors

Experimentally verified by cross-linking experiments. Substitution of cysteines in the presence of an oxidizing agent promotes cross-linking.

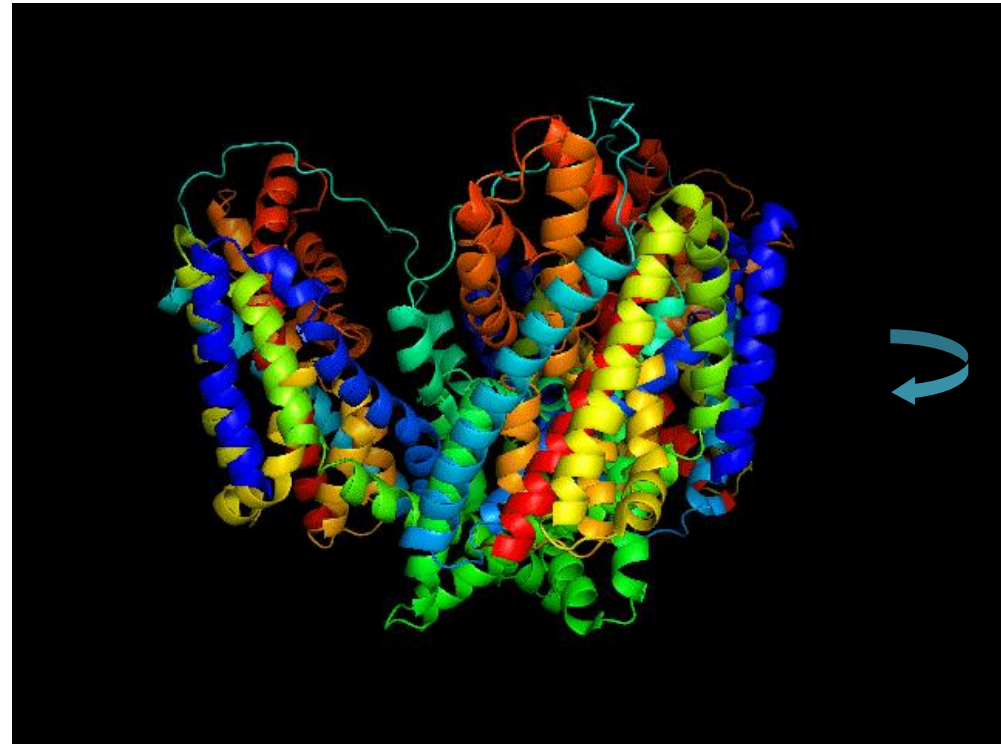


Dutta A, Krieger J, Lee JY, Garcia-Nafria J, Greger IH, Bahar I (2015) Cooperative Dynamics of Intact AMPA and NMDA Glutamate Receptors: Similarities and Subfamily-Specific Differences *Structure* 23: 1692-170

# Glutamate transporter - Glt<sub>ph</sub> structure



Trimeric aspartate transporter

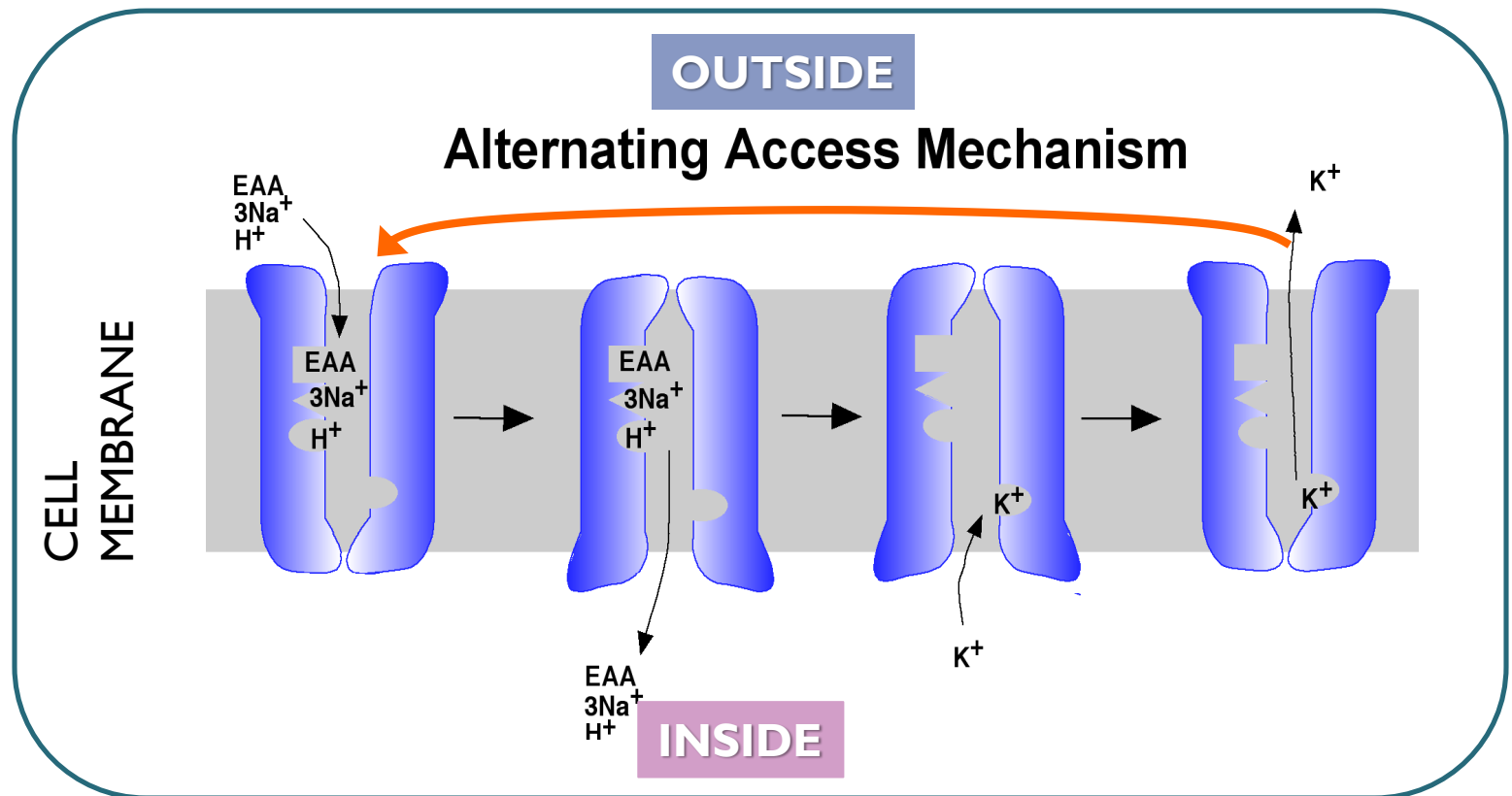


(also called EAAT – for excitatory amino acid transporter)



# Alternating-access model:

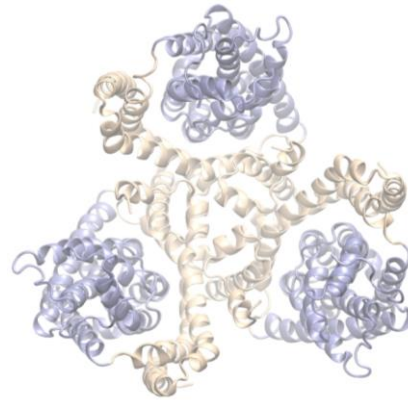
Transitions between outward-facing and inward-facing conformers



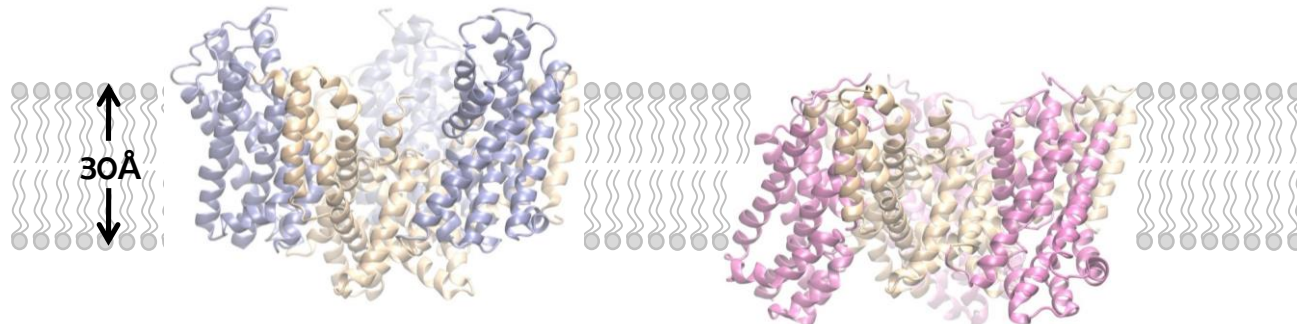
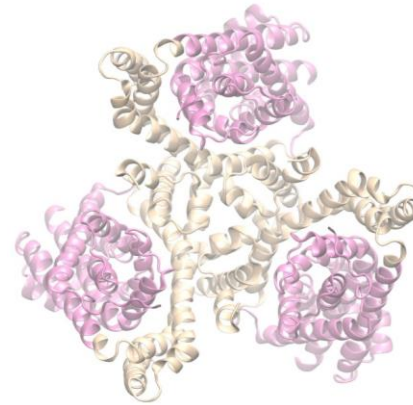
# Global transitions

Glutamate transporters – trimeric membrane proteins, each subunit composed of two domains: **scaffolding** + **transport** domains

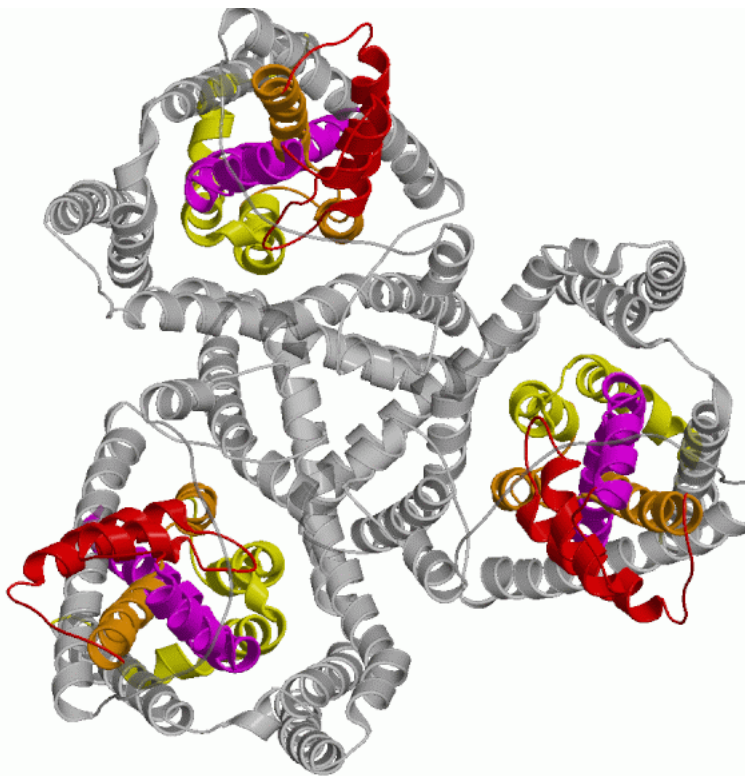
Outward Facing (OF)



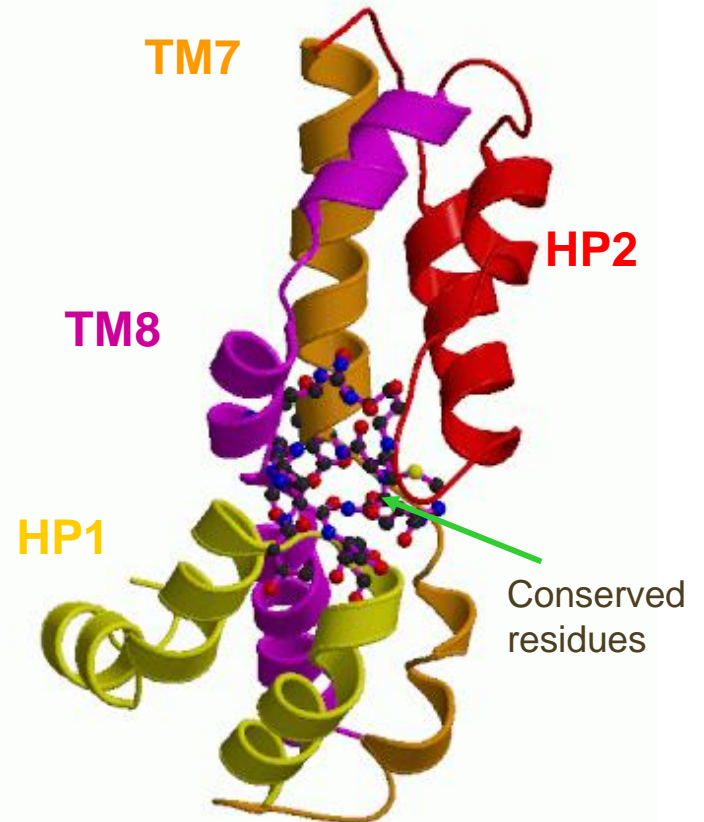
Inward Facing (IF)



Each monomer is composed of a C-terminal core and a trimerization domain

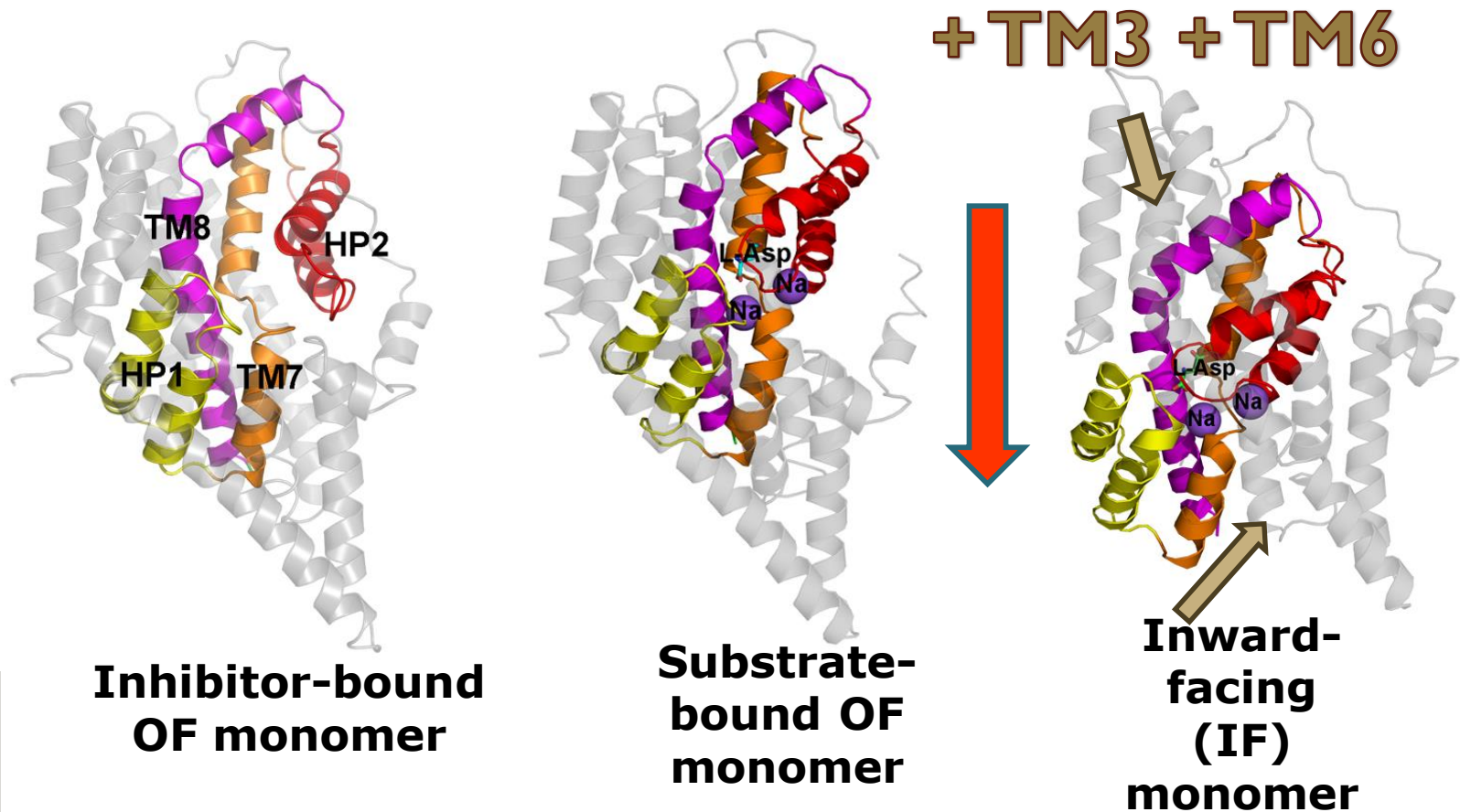


N-terminal (trimerization) domains are shown in gray; TM1-TM6)



C-terminal Core (HP1-TM7-HP2-TM8)

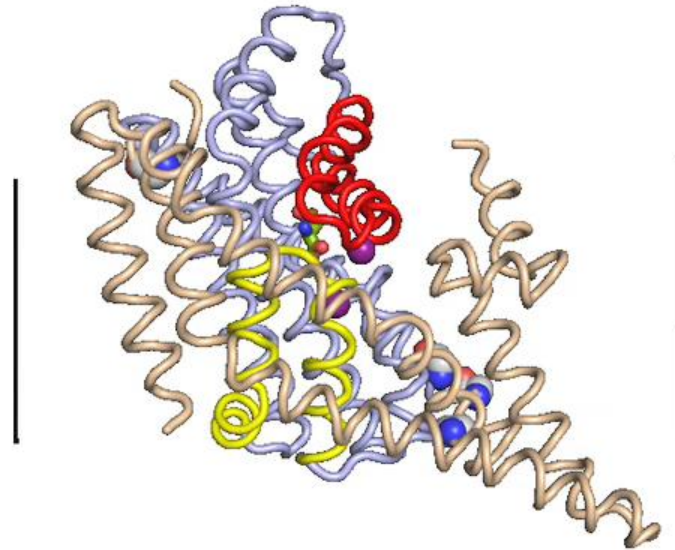
# En bloc movement of transport core



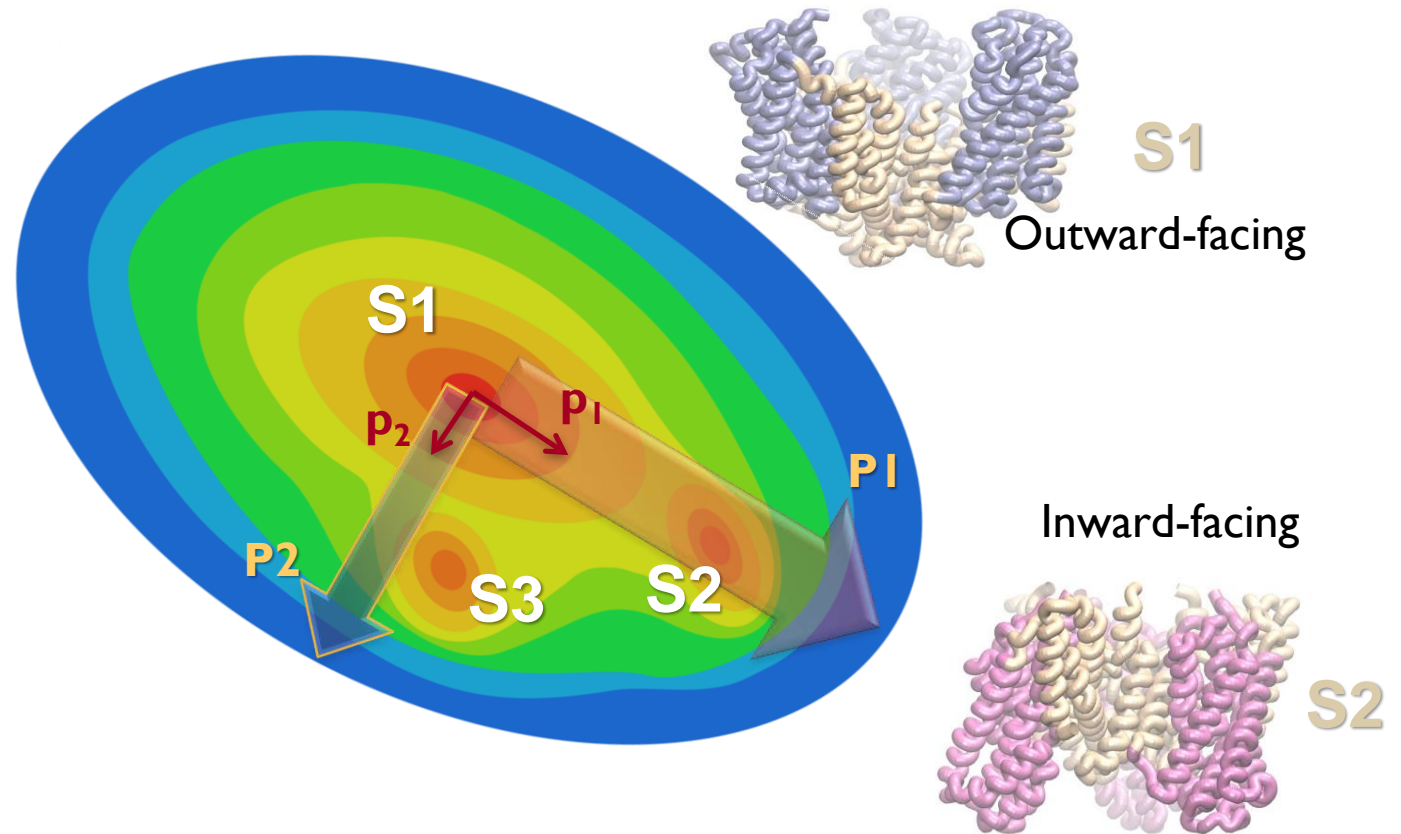
# Global transitions

Transport domain undergoes elevator-like motions, while the trimerization scaffolding domains is rigidly affixed to the membrane

Single subunit showing the transport domain moving across the membrane



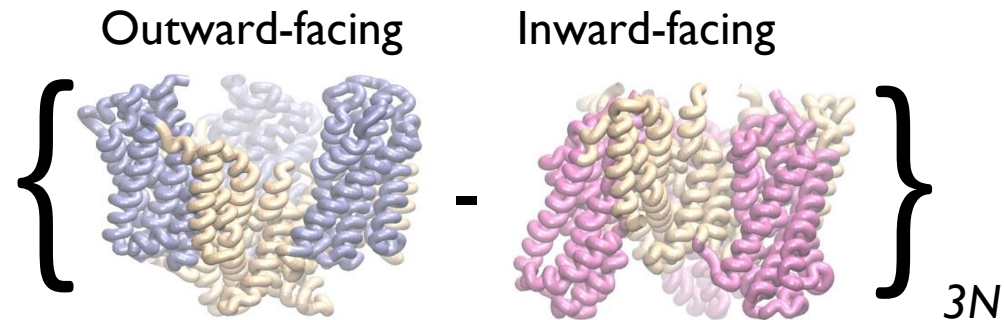
# Substates are sampled along soft modes



Is this transition along a soft mode?

# Correlation between soft modes & observed structural change

I. Evaluate of the deformation vector  $\mathbf{d}_{3N}$



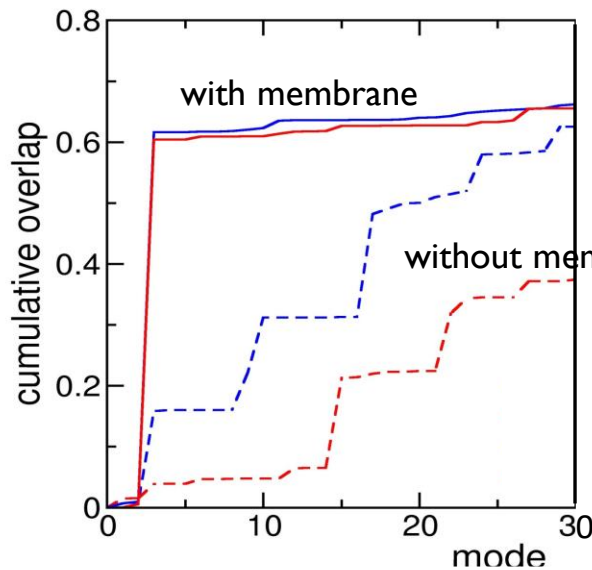
2. Calculate the **correlation cosine**  $\cos(\mathbf{v}_i, \mathbf{d})$  between each mode vector,  $\mathbf{v}_i$ , and  $\mathbf{d}$

3. **Cumulative overlap** =  $[\sum_i \cos^2(\mathbf{v}_i, \mathbf{d})]^{1/2}$

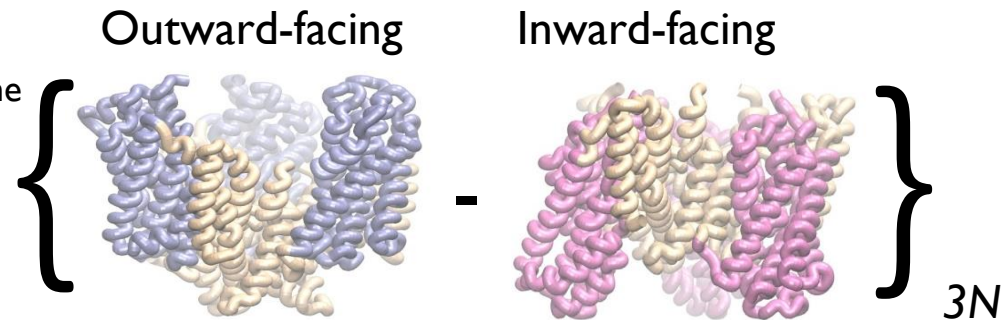
## Reference:

Lezon TR, Bahar I. (2012) Constraints imposed by the membrane selectively guide the alternating access dynamics of the glutamate transporter  $\text{Glt}_{\text{ph}}$ . *Biophys J.* **102**:1331-40.

# Correlation between soft modes & observed structural change



1. Evaluate of the deformation vector  $\mathbf{d}_{3N}$



2. Calculate the **correlation cosine**  $\cos(\mathbf{v}_i, \mathbf{d})$  between each mode vector,  $\mathbf{v}_i$ , and  $\mathbf{d}$

3. **Cumulative overlap** =  $[\sum_i \cos^2(\mathbf{v}_i, \mathbf{d})]^{1/2}$



Dr. Timothy R. Lezon

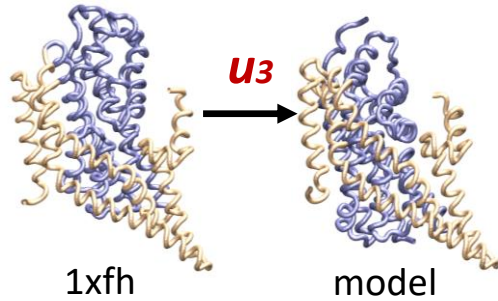
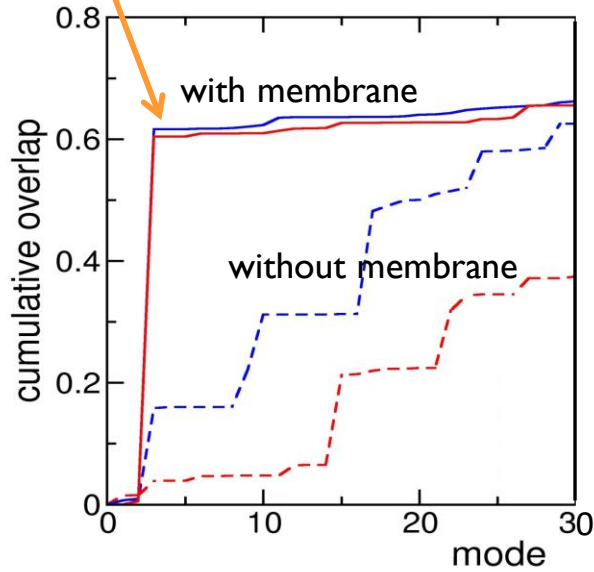
## Reference:

Lezon TR, Bahar I. (2012) Constraints imposed by the membrane selectively guide the alternating access dynamics of the glutamate transporter  $\text{Glt}_{\text{ph}}$ . *Biophys J.* **102**:1331-40.



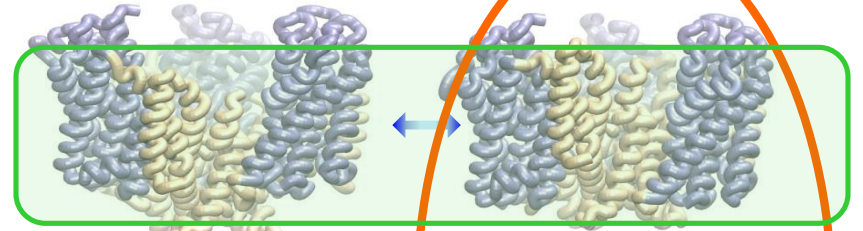
Overlap of  $> 0.6$  achieved with a single mode!

Softest nondegenerate mode out of  $> 3,000$  modes

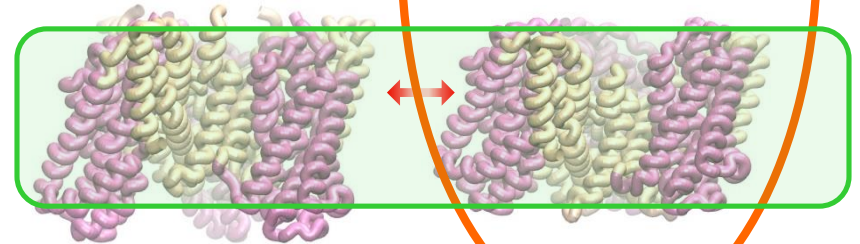


## ENM global motions

Outward-facing



Inward-facing



in the presence of lipid constraints

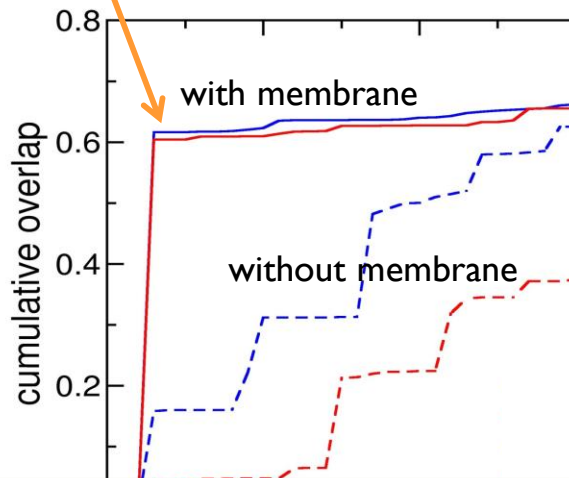
## Reference:

Lezon TR, Bahar I. (2012) Constraints imposed by the membrane selectively guide the alternating access dynamics of the glutamate transporter  $\text{Glt}_{\text{ph}}$ . *Biophys J.* **102**:1331-40.

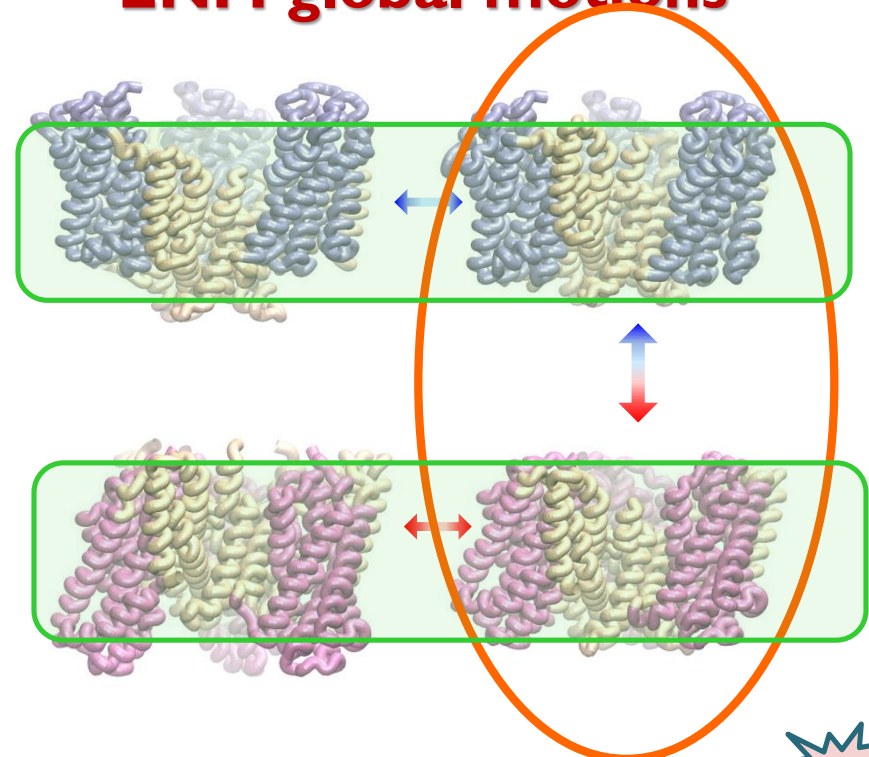
# Membrane facilitates alternating access

Overlap of  $> 0.6$  achieved with a single mode!

Softest nondegenerate mode out of  $> 3,000$  modes



## ENM global motions



in the presence of lipid constraints

If the predicted modes were 'random', each mode would contribute by  $1/3N$  to the cumulative overlap, i.e.

$$\cos(\mathbf{v}_k \cdot \mathbf{d}_{exp}) = (1/3N)^{1/2} = 0.0167$$

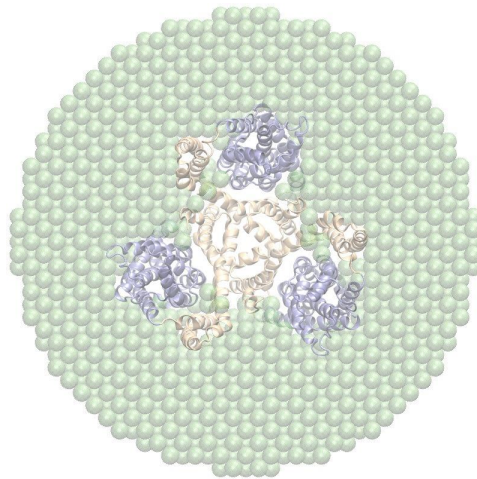
### Reference:

Lezon TR, Bahar I. (2012) Constraints imposed by the membrane selectively guide the alternating access dynamics of the glutamate transporter  $\text{Glt}_{ph}$ . *Biophys J.* **102**:1331-40.

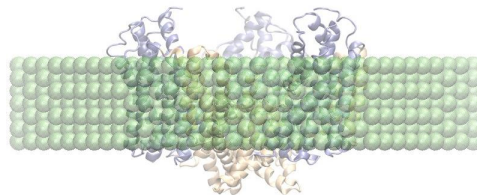
## Two approaches for including the lipid bilayer:

Explicit membrane (a network model for the membrane)

Implicit membrane (change in Hessian force constants)

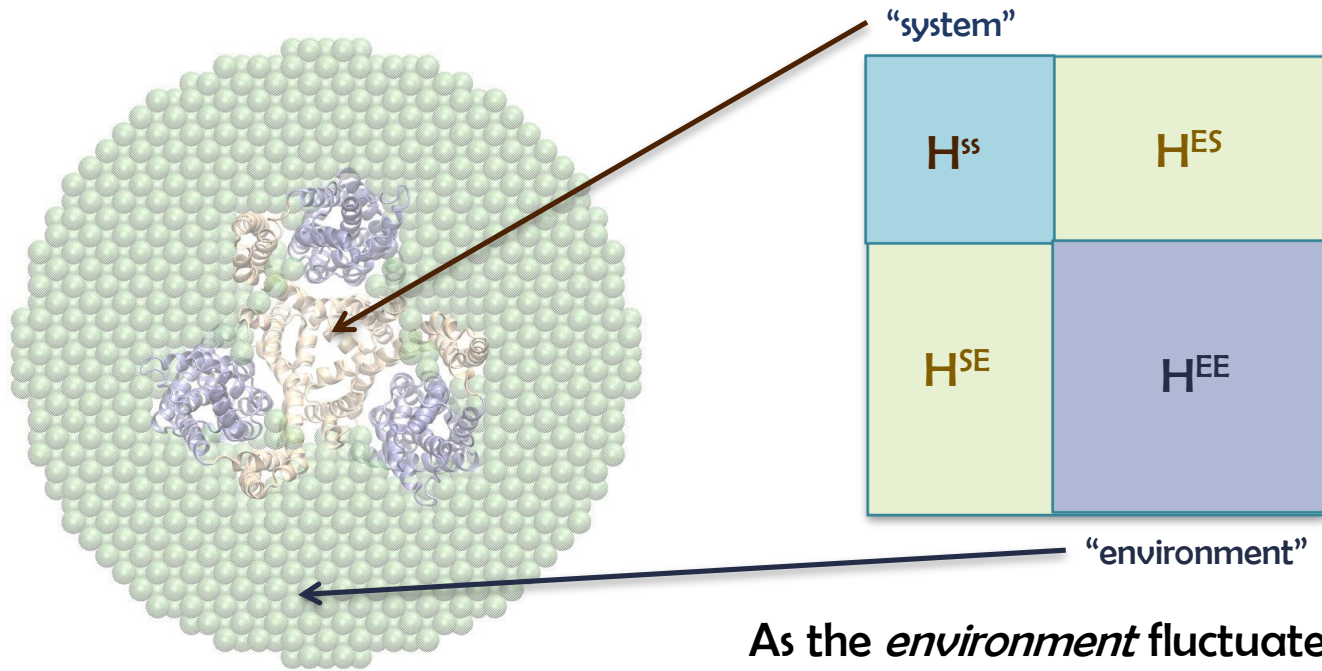


Explicit membrane top view



Explicit membrane side view

# System/environment approximation

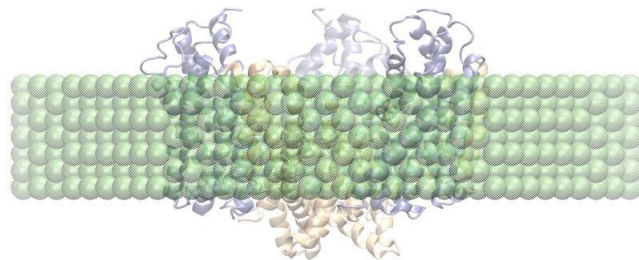


As the *environment* fluctuates randomly, the effective motion of the *system* is given by

$$V_{eff}(\mathbf{s}) = \frac{1}{2} \Delta \mathbf{s}^T (\mathbf{H}^{SS'}) \Delta \mathbf{s}$$

$$\mathbf{H}^{SS'} = \mathbf{H}^{SS} - \mathbf{H}^{SE} (\mathbf{H}^{EE})^{-1} \mathbf{H}^{ES}$$

reduceModel()



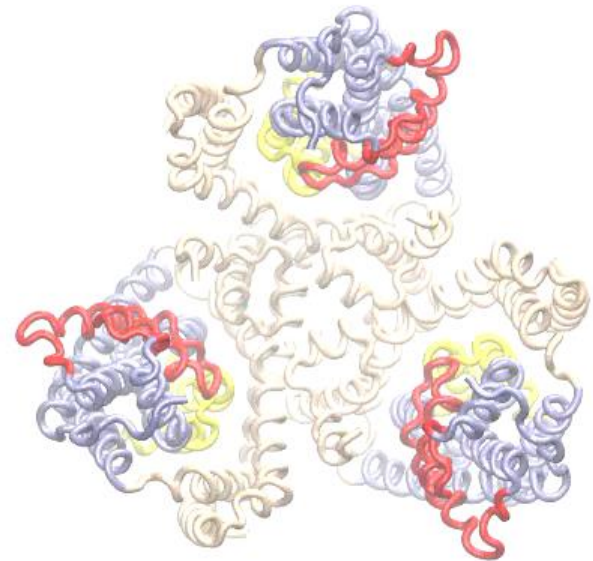
# Implicit model for membrane effect

$$\mathbf{H}_{ij} = -\frac{\gamma}{(R_{ij}^0)^2} \begin{bmatrix} (x_{ij}^0)^2 & x_{ij}^0 y_{ij}^0 & x_{ij}^0 z_{ij}^0 \\ x_{ij}^0 y_{ij}^0 & (y_{ij}^0)^2 & y_{ij}^0 z_{ij}^0 \\ x_{ij}^0 z_{ij}^0 & y_{ij}^0 z_{ij}^0 & (z_{ij}^0)^2 \end{bmatrix}$$

Altered radial force constants:

$$\mathbf{H}_{ij} = -(R_{ij}^0)^{-2} \begin{bmatrix} (x_{ij}^0 \sqrt{\gamma_x})^2 & x_{ij}^0 y_{ij}^0 \sqrt{\gamma_x \gamma_y} & x_{ij}^0 z_{ij}^0 \sqrt{\gamma_x \gamma_z} \\ x_{ij}^0 y_{ij}^0 \sqrt{\gamma_x \gamma_y} & (y_{ij}^0 \sqrt{\gamma_y})^2 & y_{ij}^0 z_{ij}^0 \sqrt{\gamma_y \gamma_z} \\ x_{ij}^0 z_{ij}^0 \sqrt{\gamma_x \gamma_z} & y_{ij}^0 z_{ij}^0 \sqrt{\gamma_y \gamma_z} & (z_{ij}^0 \sqrt{\gamma_z})^2 \end{bmatrix}$$

$$\mathbf{H}_{ij} = -\frac{g}{(R_{ij}^0)^2} \begin{matrix} \hat{e} & \hat{e} & \hat{e} & \hat{u} \\ \hat{e} & (x_{ij}^0)^2 & x_{ij}^0 y_{ij}^0 & cx_{ij}^0 z_{ij}^0 \\ \hat{e} & x_{ij}^0 y_{ij}^0 & (y_{ij}^0)^2 & cy_{ij}^0 z_{ij}^0 \\ \hat{e} & cx_{ij}^0 z_{ij}^0 & cy_{ij}^0 z_{ij}^0 & (cz_{ij}^0)^2 \\ \hat{e} & \hat{e} & \hat{e} & \hat{e} \end{matrix}$$



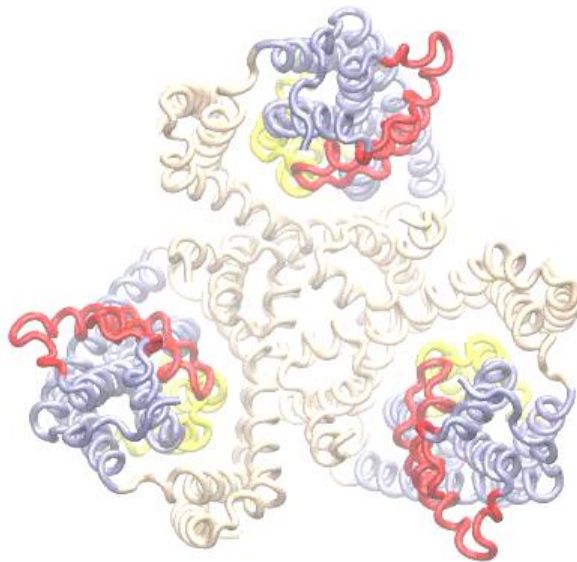
RTB.buildHessian()

Lezon & Bahar. Biophys J 102 (2012).

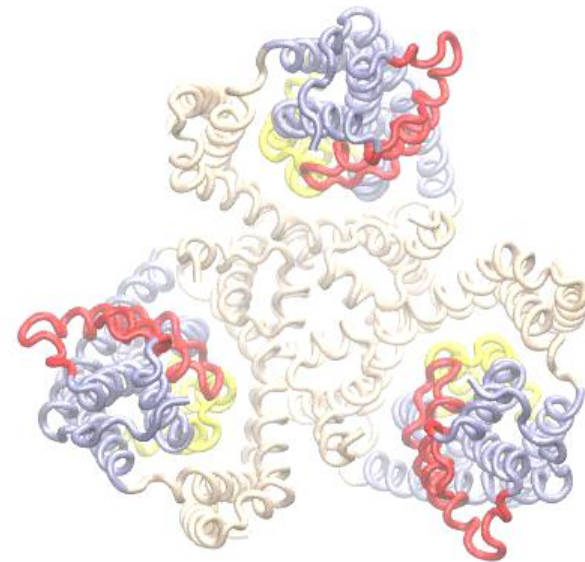
# Lipid bilayer favors elevator-like motions



Dr. Timothy R Lezon



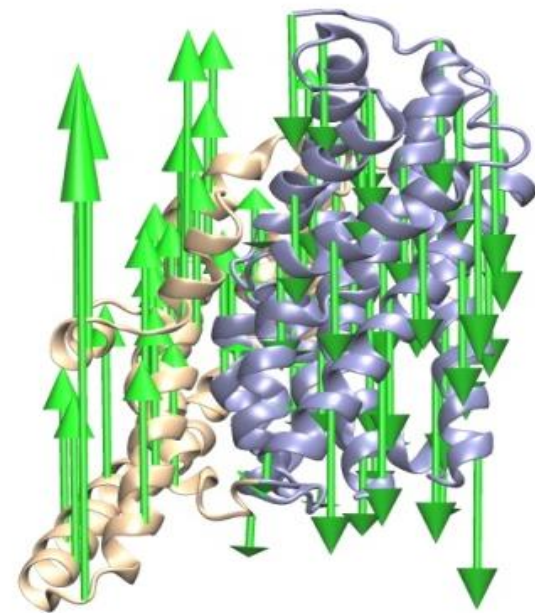
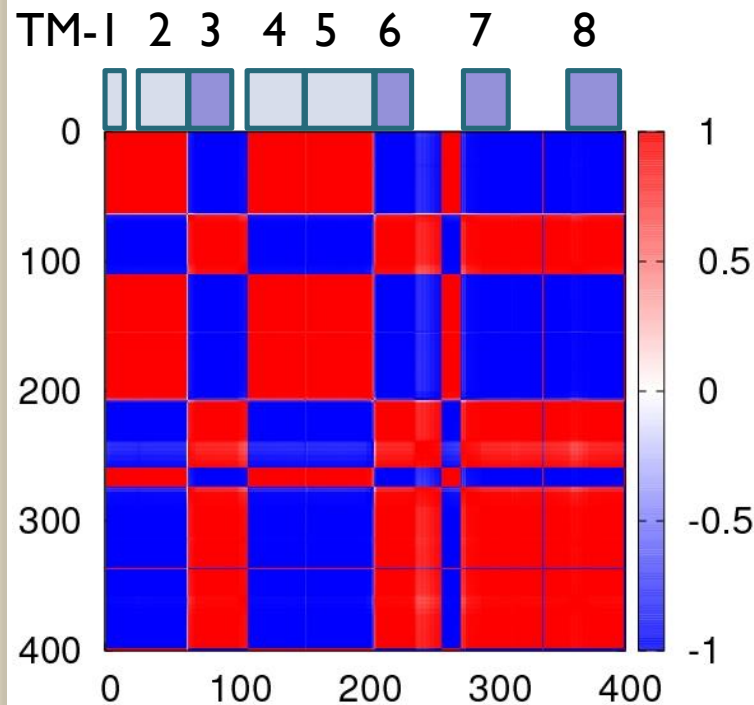
ANM in the absence of membrane



ANM in the presence of membrane

# DOMAIN SEPARATION PREDICTED BY GNM

TM3 and TM6 form an integral part of the transport core (TM7, TM8, HP1 and HP2)



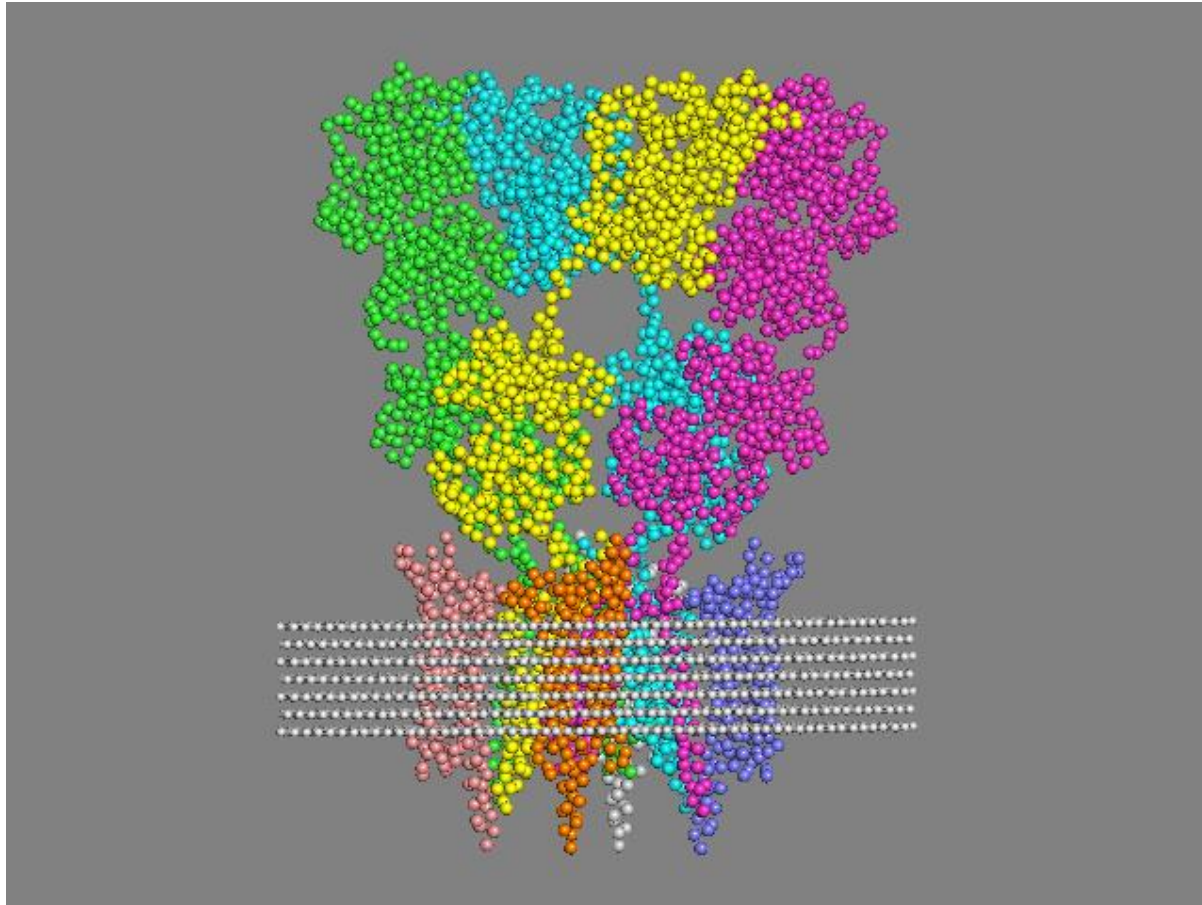
TM1, TM2,  
TM4, TM5

TM3, TM6,  
+ transport core

Reference:

Lezon TR, Bahar I. (2012) Constraints imposed by the membrane selectively guide the alternating access dynamics of the glutamate transporter  $Glt_{ph}$ . *Biophys J.* **102**:1331-40.

# MembrANM - DynOmics

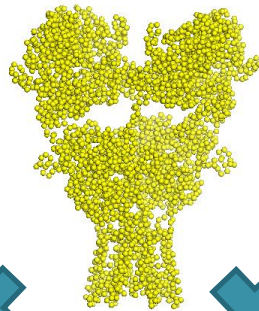




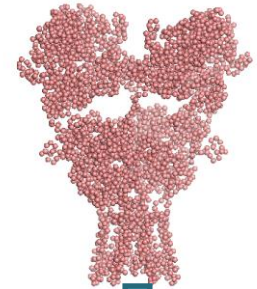
# Coupled motions of AMPAR and lipid bilayer

Motions without membrane

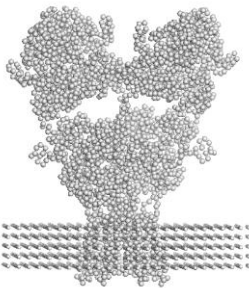
Mode4



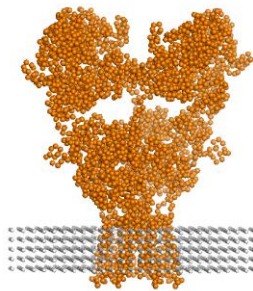
mode5



mode6

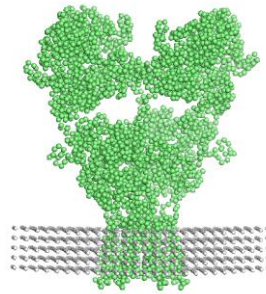


mode8

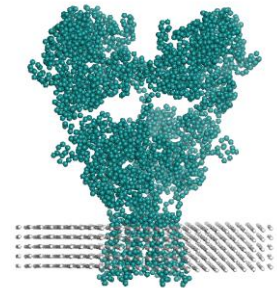


New mode

mode9

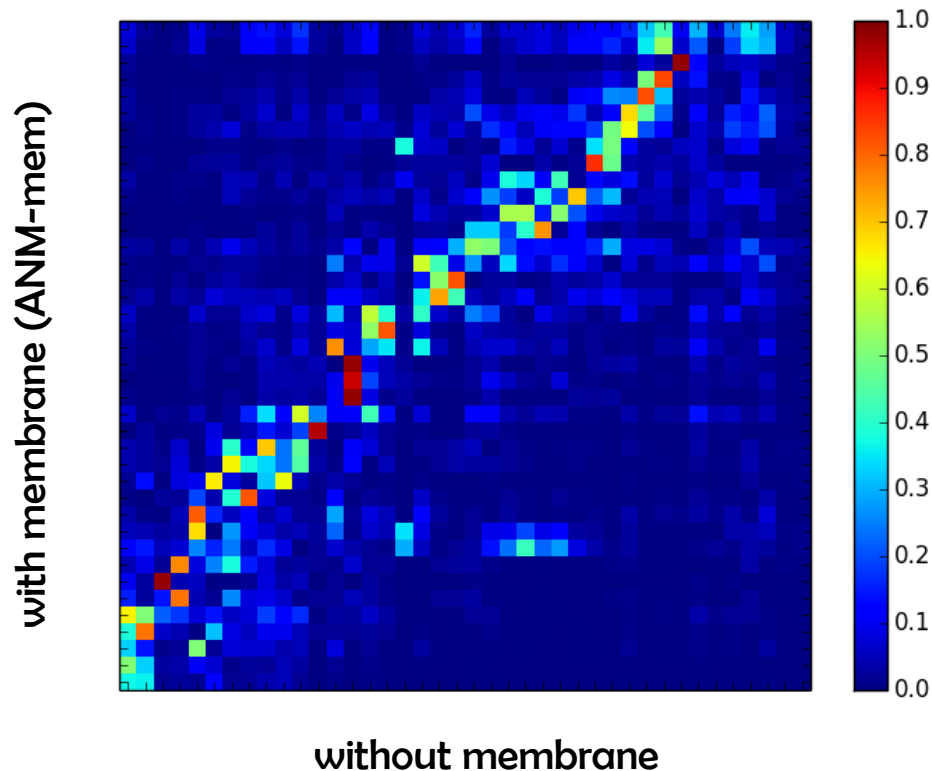


mode10



Motions with membrane

# Comparison of mode shapes



In the presence of membrane:

- Some intrinsic motions are preserved (*red*)
- Others are altered (*yellow*)
- New motions (mainly dominated by membrane fluctuations) emerge (blue rows)
- Diagonal shift due to new modes in the membrane



# Druggability

# Druggable Genome

A small subset of are 'disease-modifying' – and not all of them are druggable

Human Genome (21,000) genes

Druggable genome  
3,000 genes

430+ kinases  
600+ GPCRs

70+ kinases  
100+ GPCRs

**Drug  
Targets**  
600-1,500

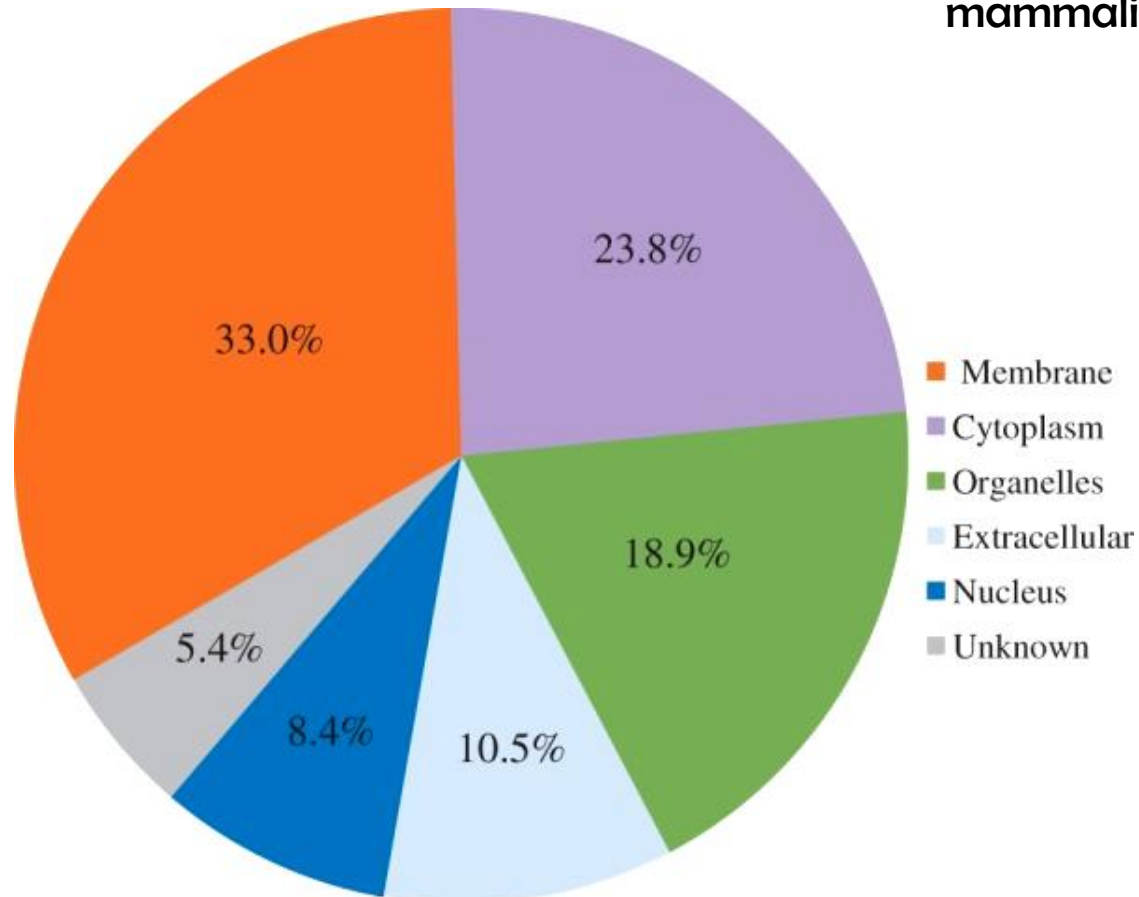
Disease-related genes  
~3,000 genes

# A few numbers...

- Only 2% of human proteins interact with currently approved drugs.
- 10-15% of human proteins are disease-modifying
- 10-15% are druggable
- 5% are both disease-modifying and druggable

# Subcellular distribution of 1,362 druggable targets

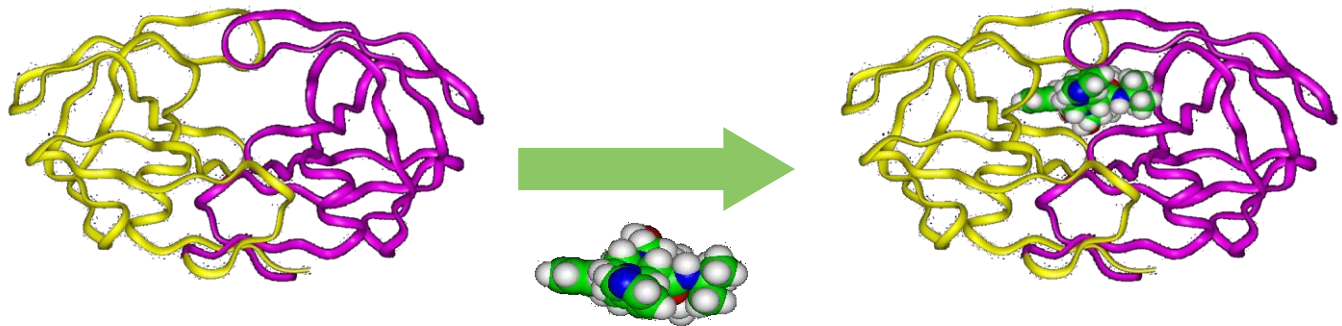
among four mammalian species.



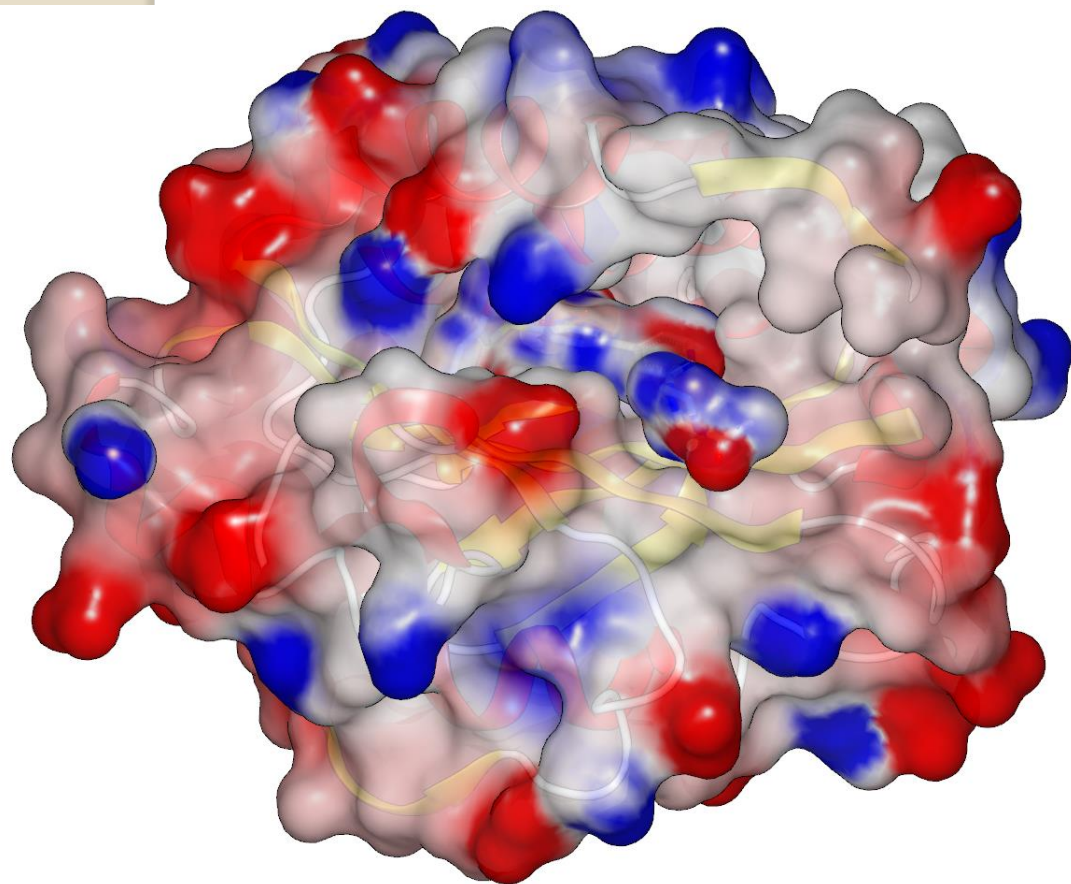
# Rational Design of Inhibitors

3D structure of the target is used for

- Visual inspection/molecular graphics
- Docking (of small molecules or fragments thereof)
- *De novo* methods
- Receptor properly mapping + database searching



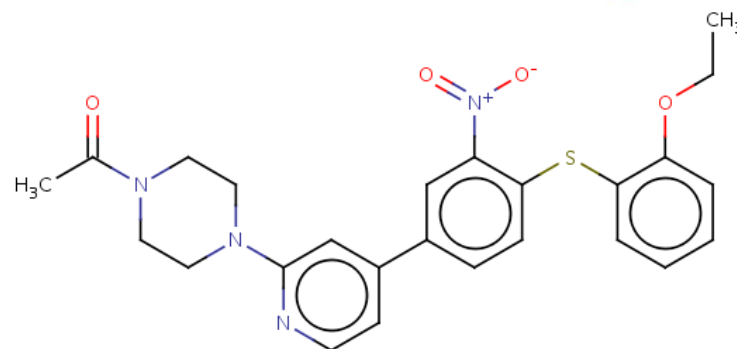
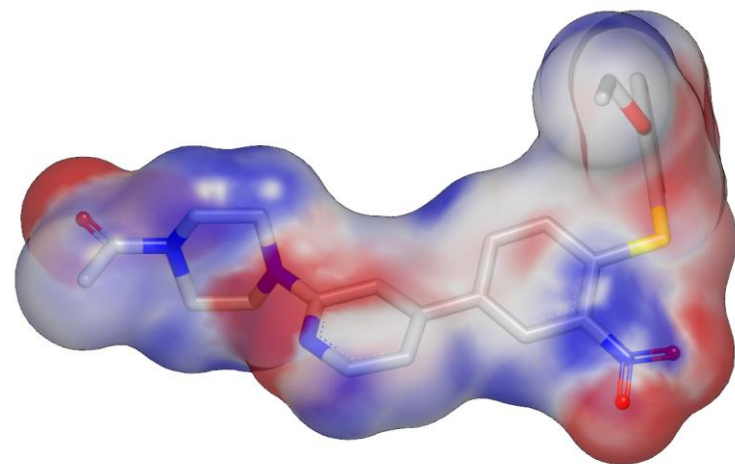
# Druggable or not?



**Lfa1** - a leukocyte glycoprotein that promotes intercellular adhesion and binds intercellular adhesion molecule 1

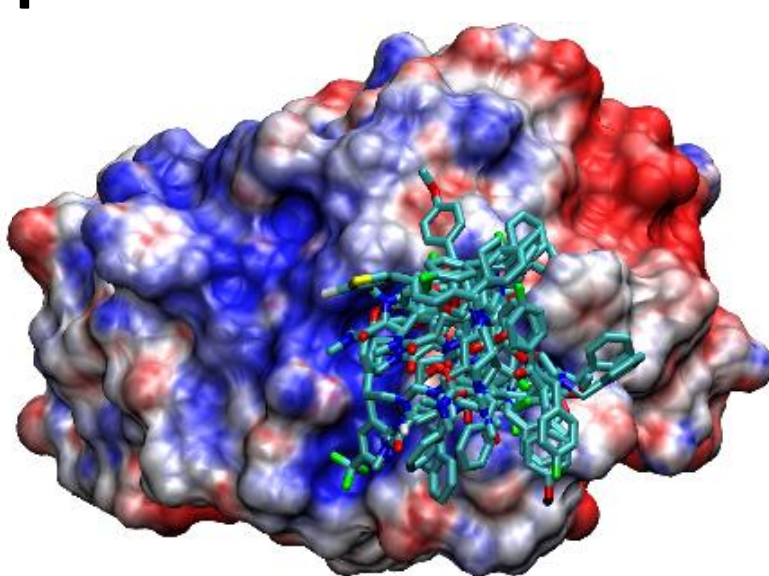
## Active site druggability:

- Best known  $K_d$  18.3 nM
- Simulation 0.03-0.5 nM

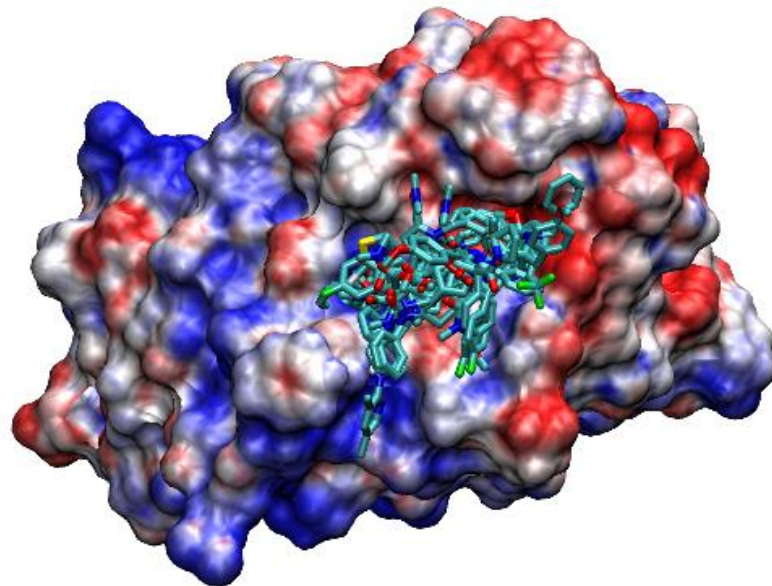




# Some proteins do not present well-defined pockets



**MKP-1**



**VHR**

A problem:

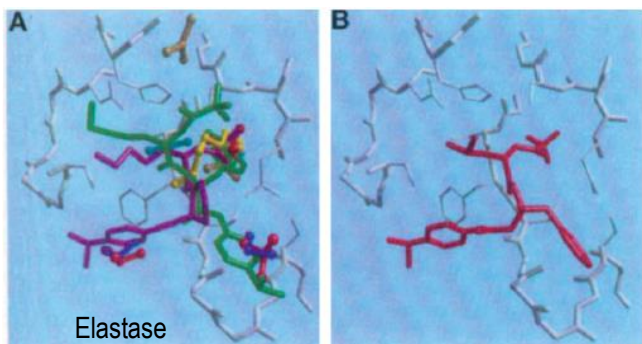
Hard to discriminate between different binding compounds/poses for a given target if the surface does not present suitable pockets

"Structurally Unique Inhibitors of Human Mitogen-activated Protein Kinase Phosphatase-1 Identified in a Pyrrole Carboxamide Library." Lazo et al (2007) J Pharmacol Exp Ther.

# Druggability from Experiments

## • X-ray crystallography

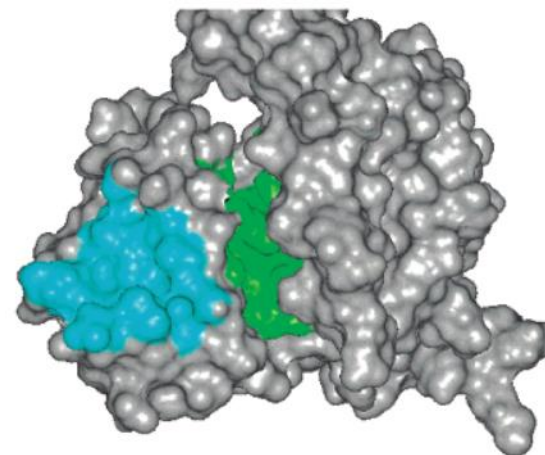
- protein structure is solved in presence of small organic molecules



Mattos and Ridge, *Nat Biotechnology*, 1996

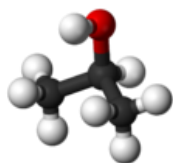
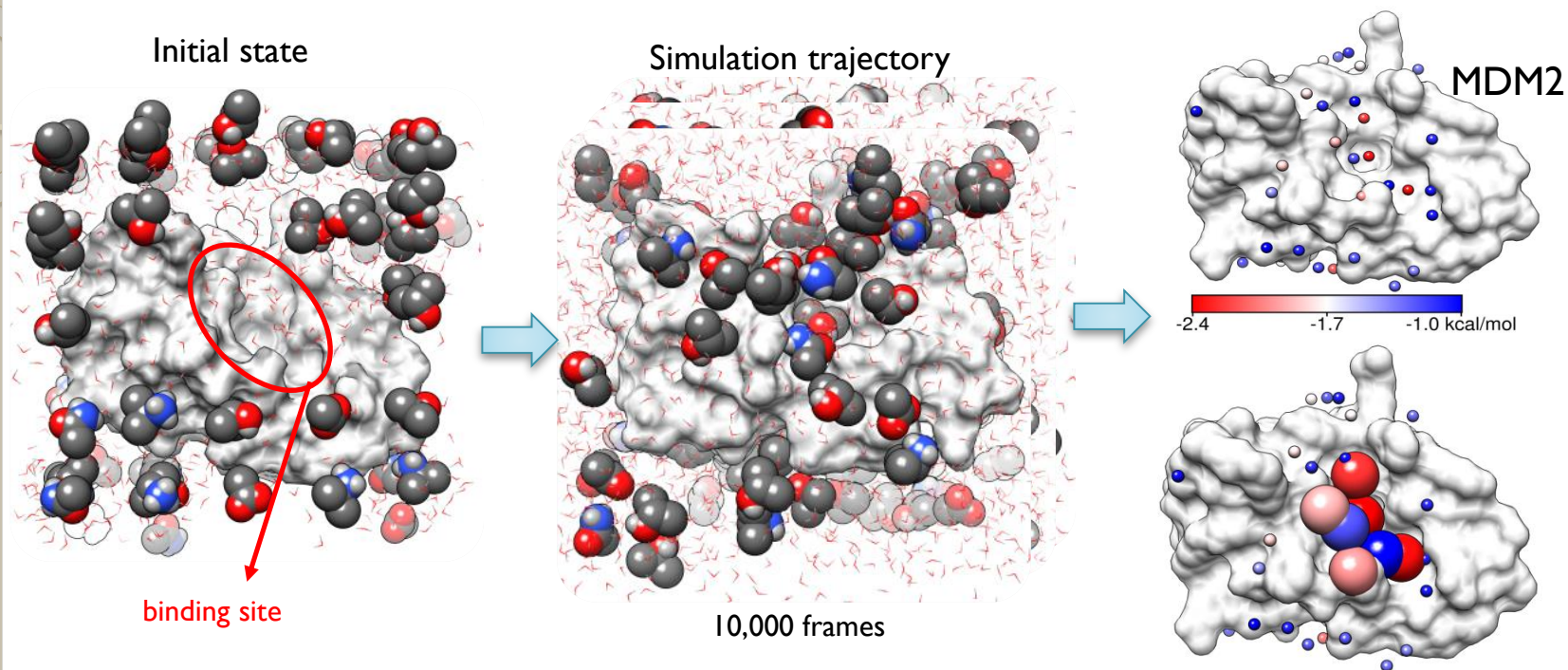
## • NMR screening

- compounds from a fragment-library are screened as mixtures of 20-30 compounds, druggability is calculated from chemical shift perturbations

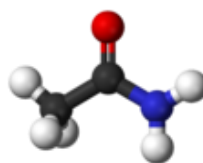


Hajduk et al., *J Med Chem*, 2005

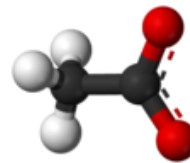
# Druggability Simulations



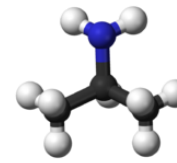
Isopropanol  
(observed in 57% of drugs)



Acetamide  
(21%)



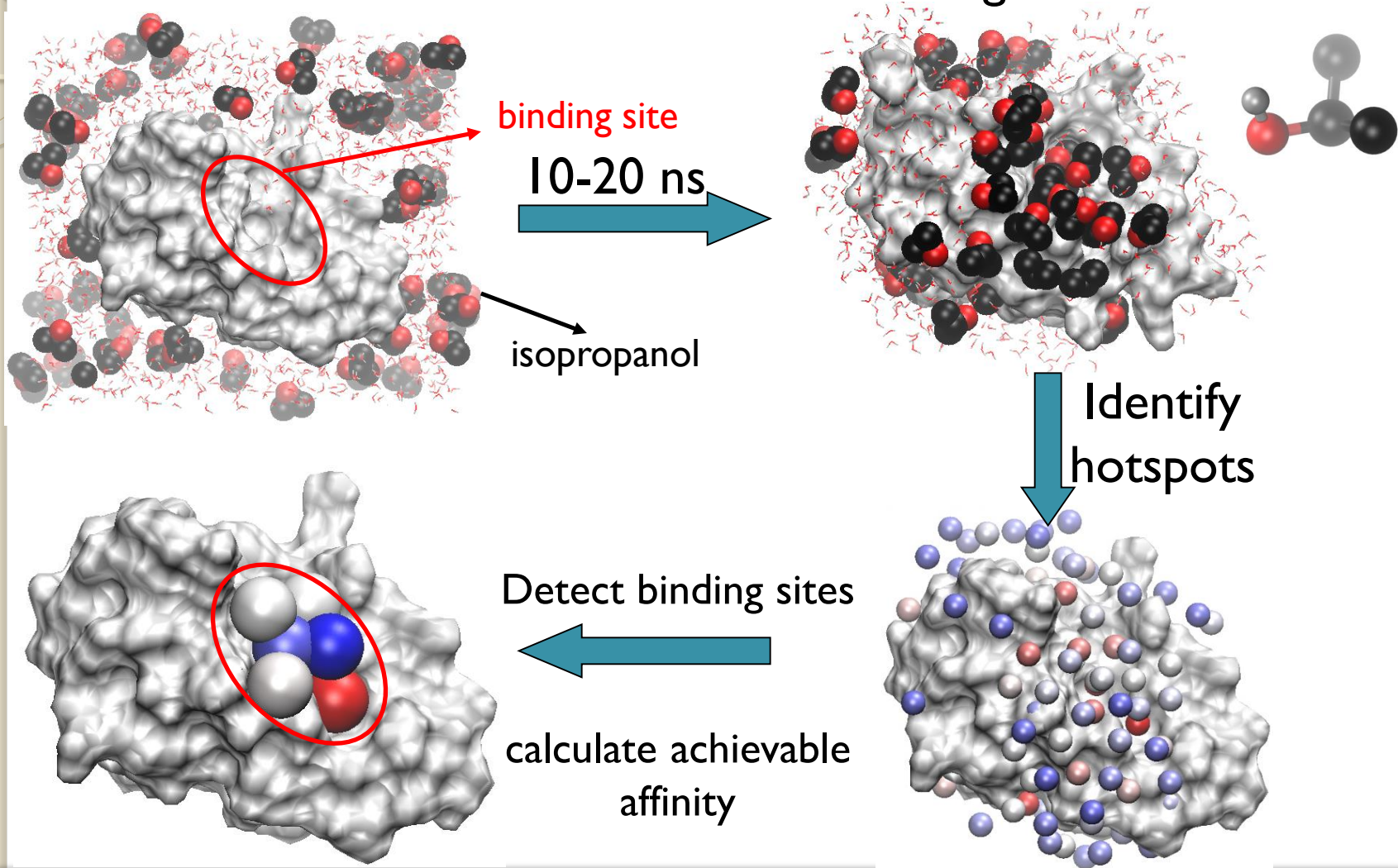
Acetate (-1)  
(21%)



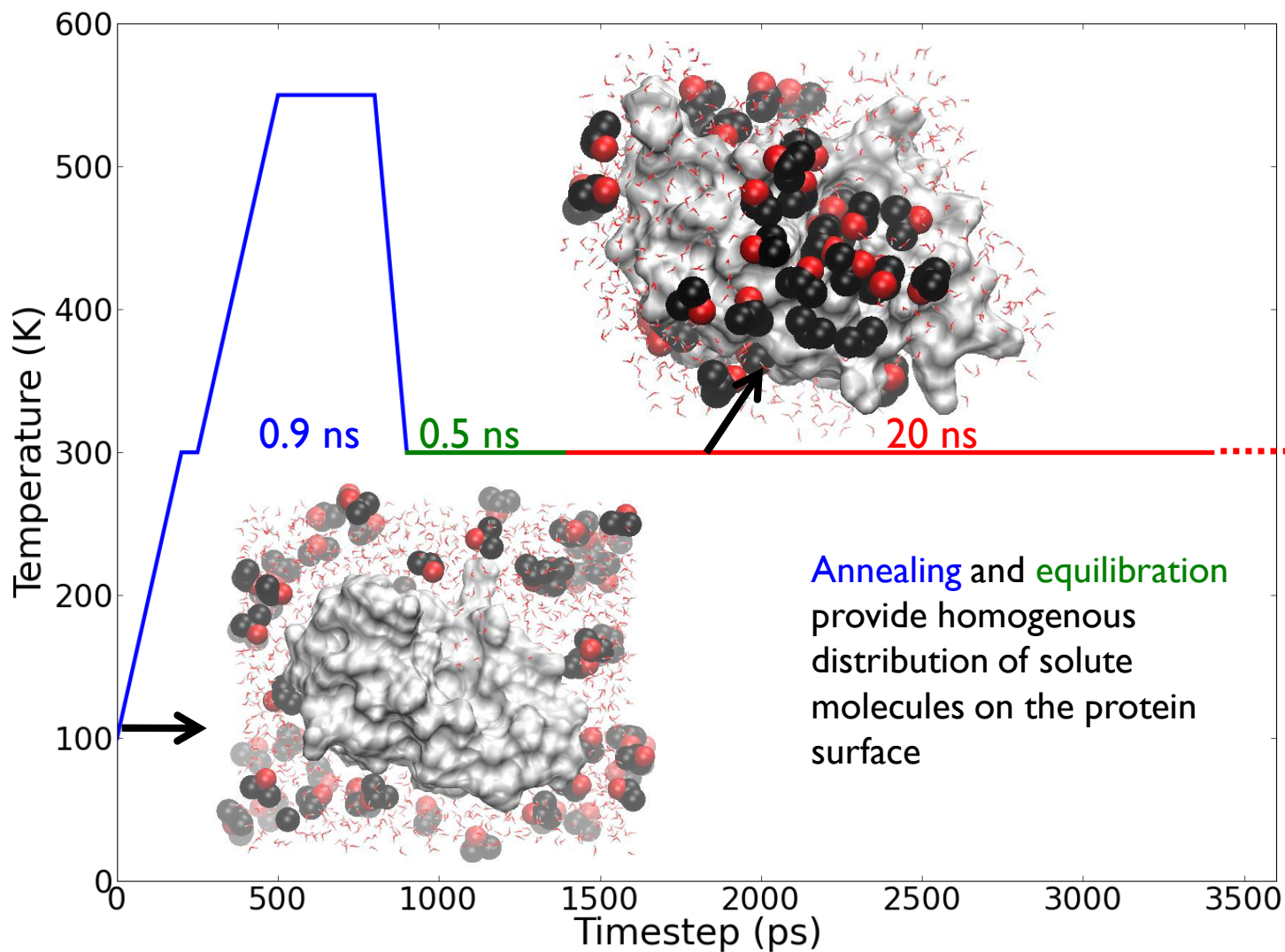
Isopropylamine (+1)  
(25%)

# Methodology Overview

From MD simulations to achievable drug affinities



# Annealing, Equilibration, Simulation



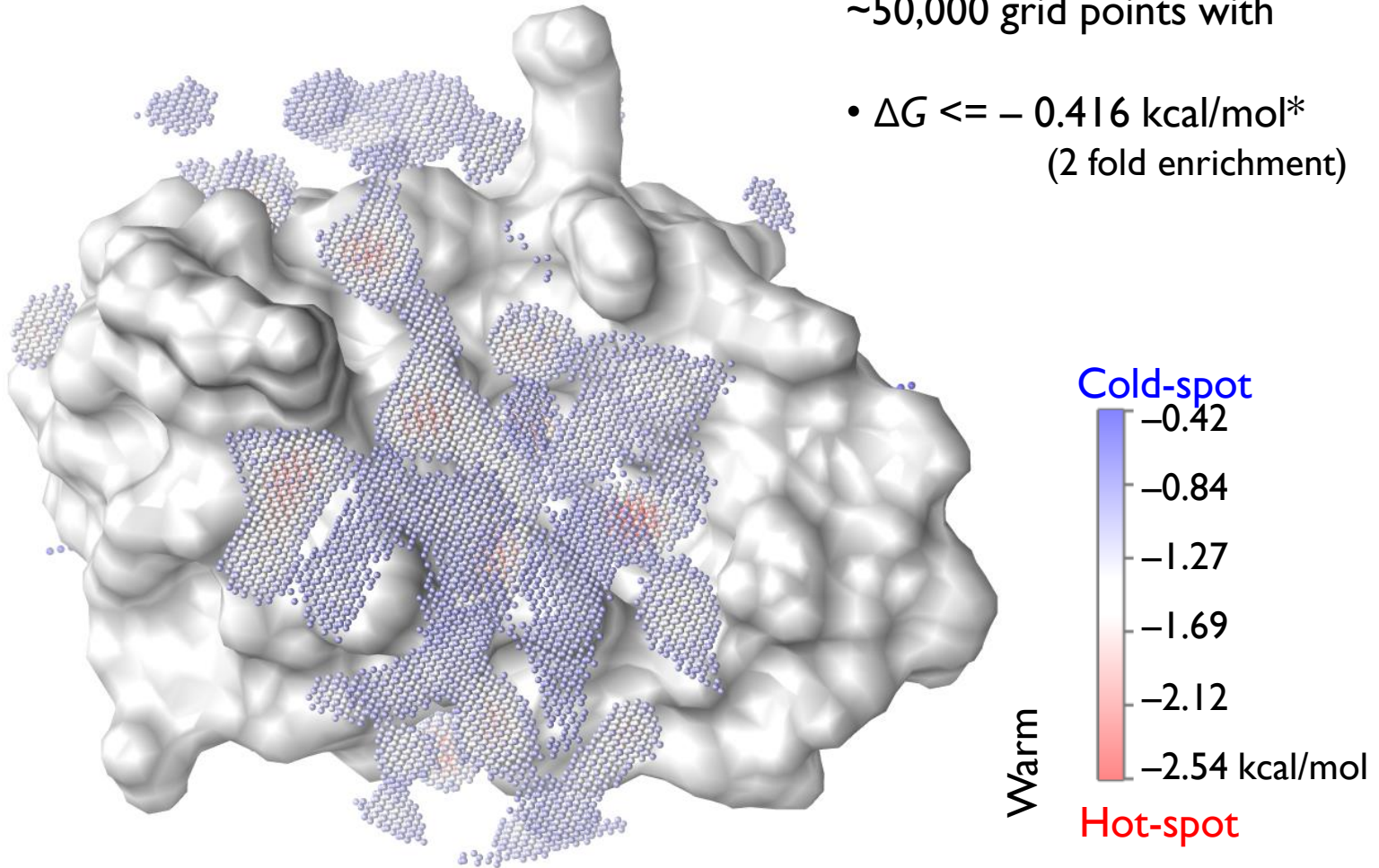
NAMD2 with CHARMM force field was used for simulations.

# Isopropanol Binding Spots

$\Delta G$  grid is mapped onto the protein structure

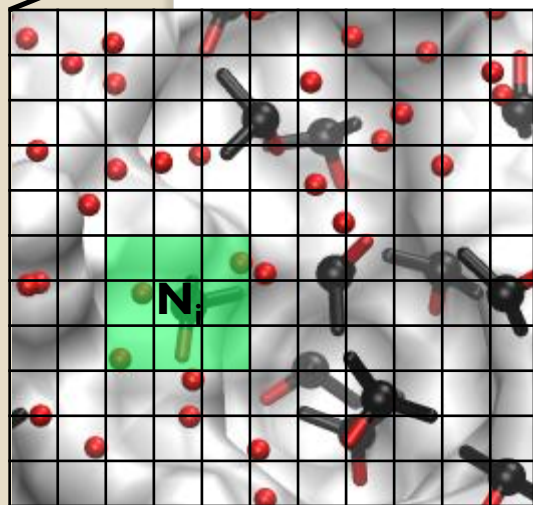
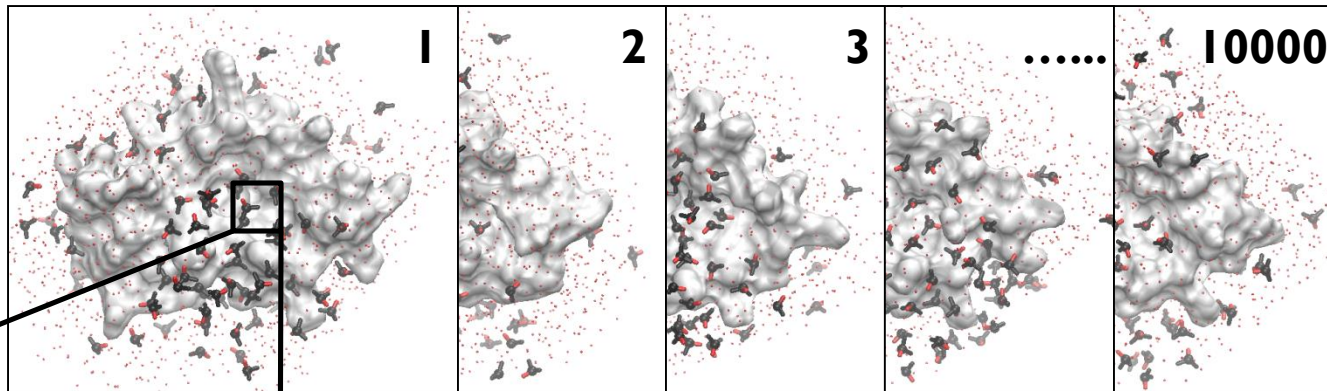
~50,000 grid points with

- $\Delta G \leq -0.416$  kcal/mol\*  
(2 fold enrichment)



# Free Energy of Binding for Isopropanol

Assuming that MD sampling converged to a **Boltzmann ensemble**

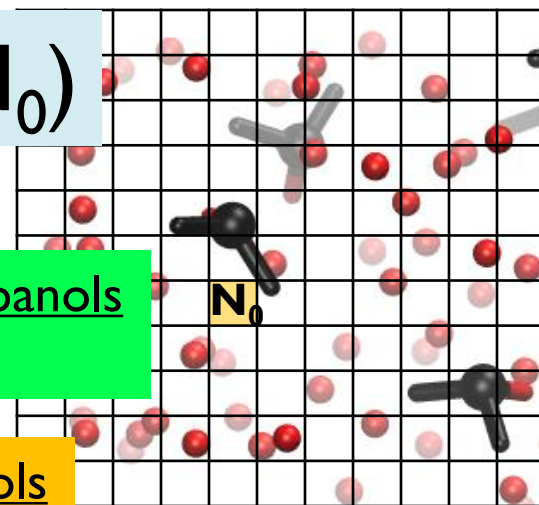


0.5 Å (not to scale)

$$\Delta G_i = -RT \ln(N_i/N_0)$$

$N_i$  = observed number of isopropanols  
(# of frames) \* (# of cubes)

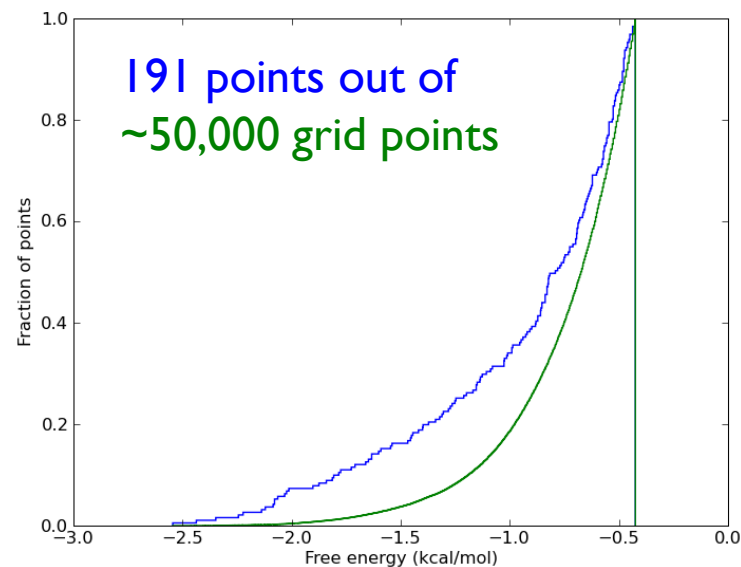
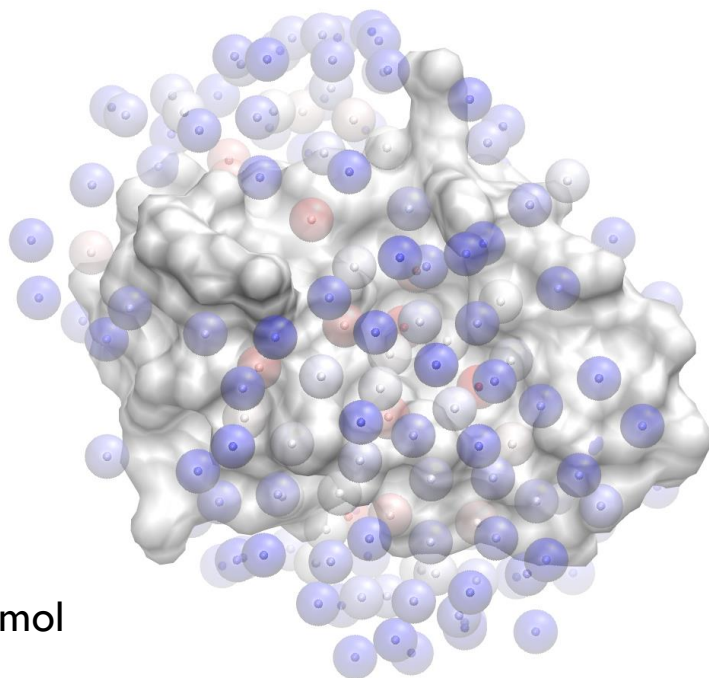
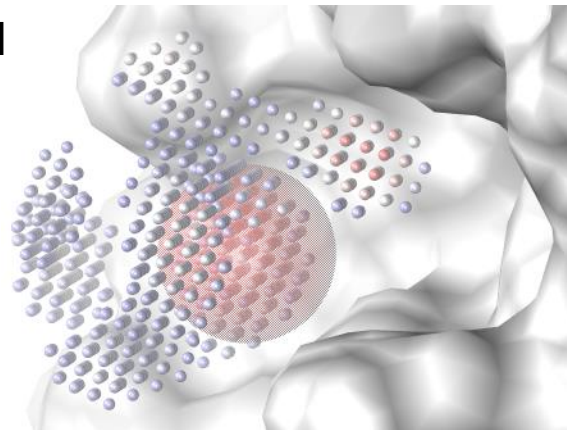
$N_0$  = total number of isopropanols  
total number of frames



$N_i$  corresponds to the central highlighted grid element;  
number of cubes is introduced if multiple cubes are occupied by a single isopropanol

# Selecting Isopropanol Binding Spots

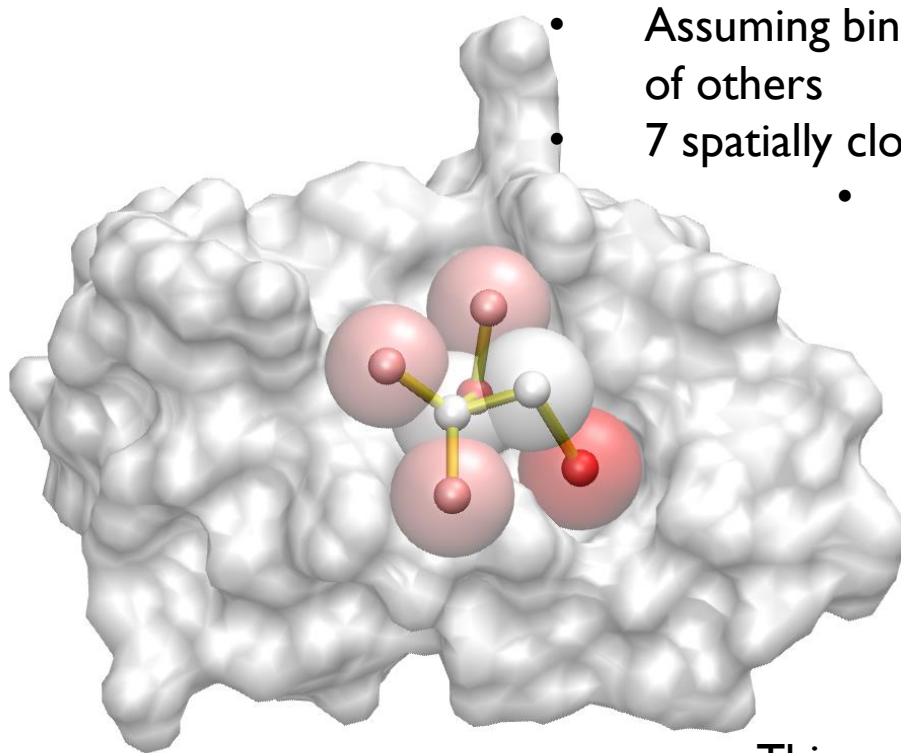
1. Grid element with lowest  $\Delta G$  value is selected
2. Other elements within **4 Å** are removed (elements inside the red sphere  $\rightarrow$ )
3. 1 and 2 are repeated until no more points are left to remove





# Affinity of a Drug-size Molecule

A heuristic approach for calculating achievable free energy of binding



- Assuming binding of an isopropanol is independent of others

- 7 spatially close binding spots are selected

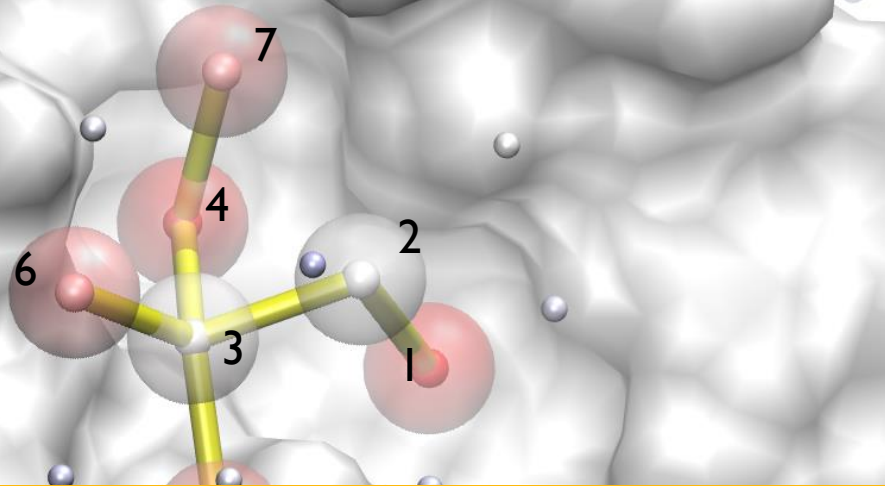
- The sum of  $\Delta G_{binding}$  of individual points is considered as a binding free energy estimate that is achievable by a drug-like molecule

This way, the highest affinity we can observe is 5 fM ( $10^{-15}$ ).

# MDM2: p53 binding site

p53 peptide key interactions (X-ray)

Highest affinity solution (7 points)



The top solution is in the protein-protein interaction site

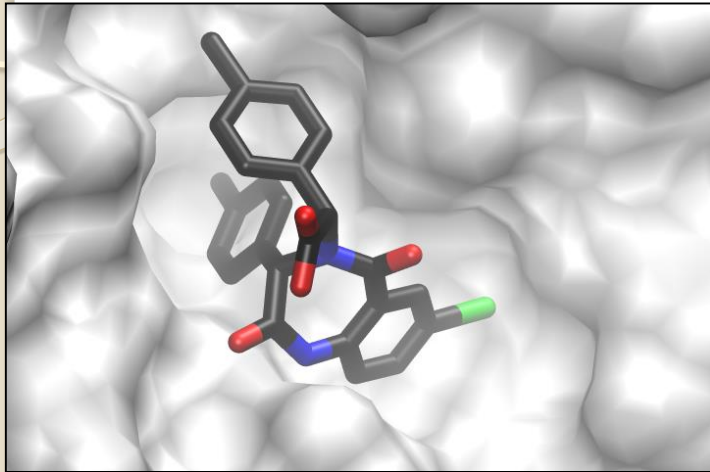
Numbers indicate the order that hot spots were merged by the growing algorithm

Predicted binding affinity range : **0.05-0.3 nM**

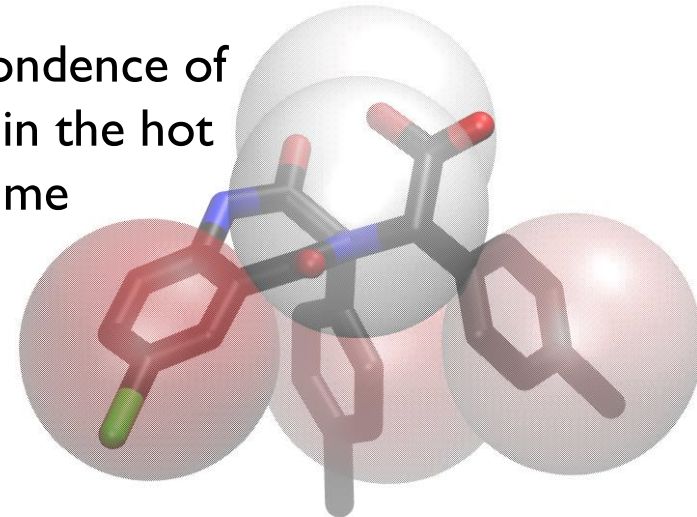
Predicted max. affinity by Seco et al. : **0.02 nM**

# MDM2: p53 binding site

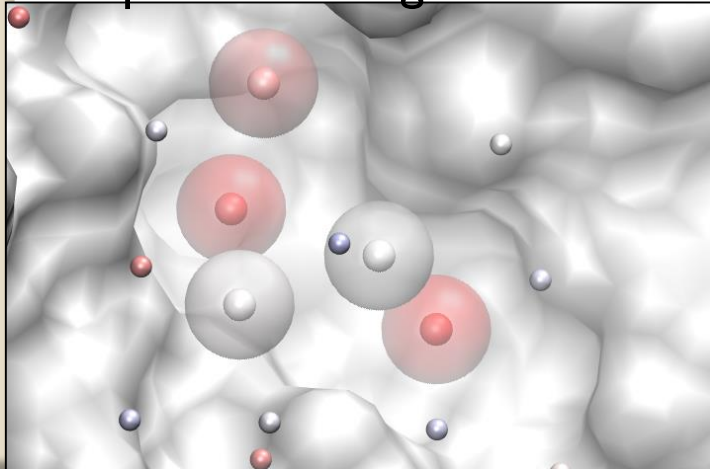
An inhibitor that disrupts p53 binding



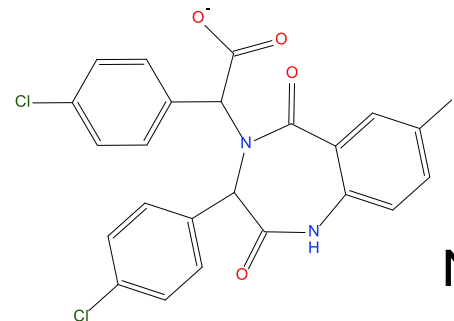
Correspondence of inhibitor in the hot spot volume



Hot spots matching this inhibitor

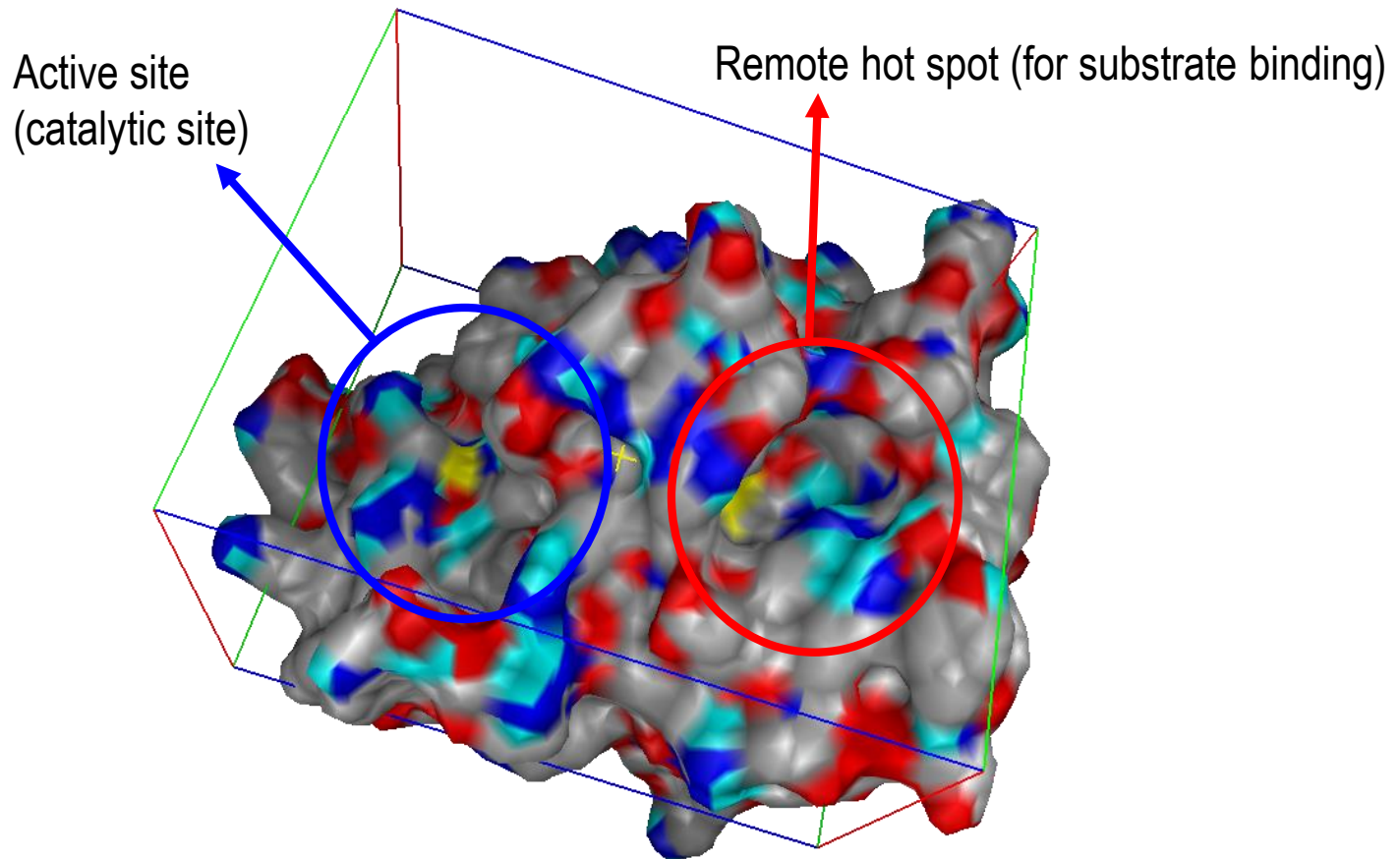


Predicted  $K_d$ : **47 nM**  
Known  $K_d$  : **80 nM**

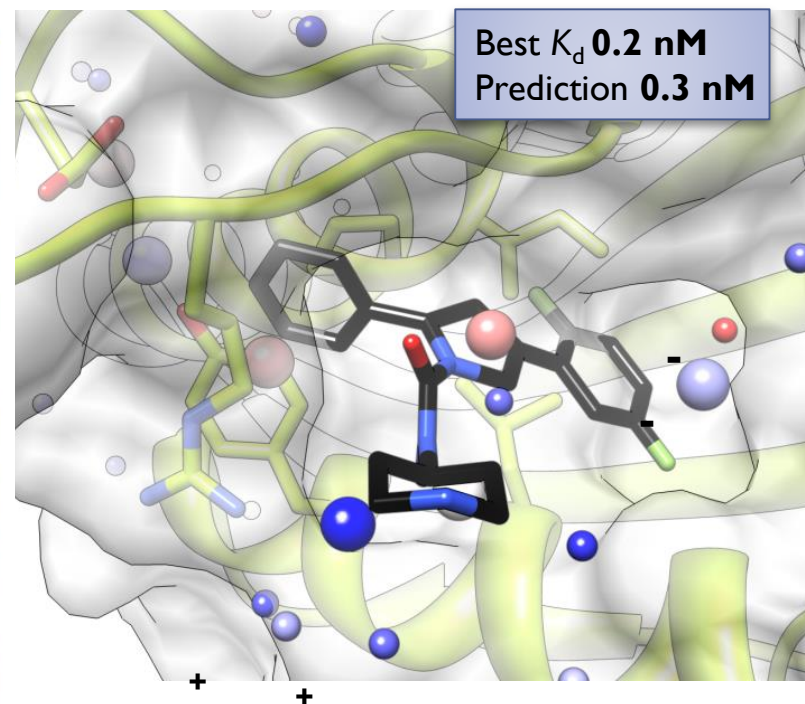
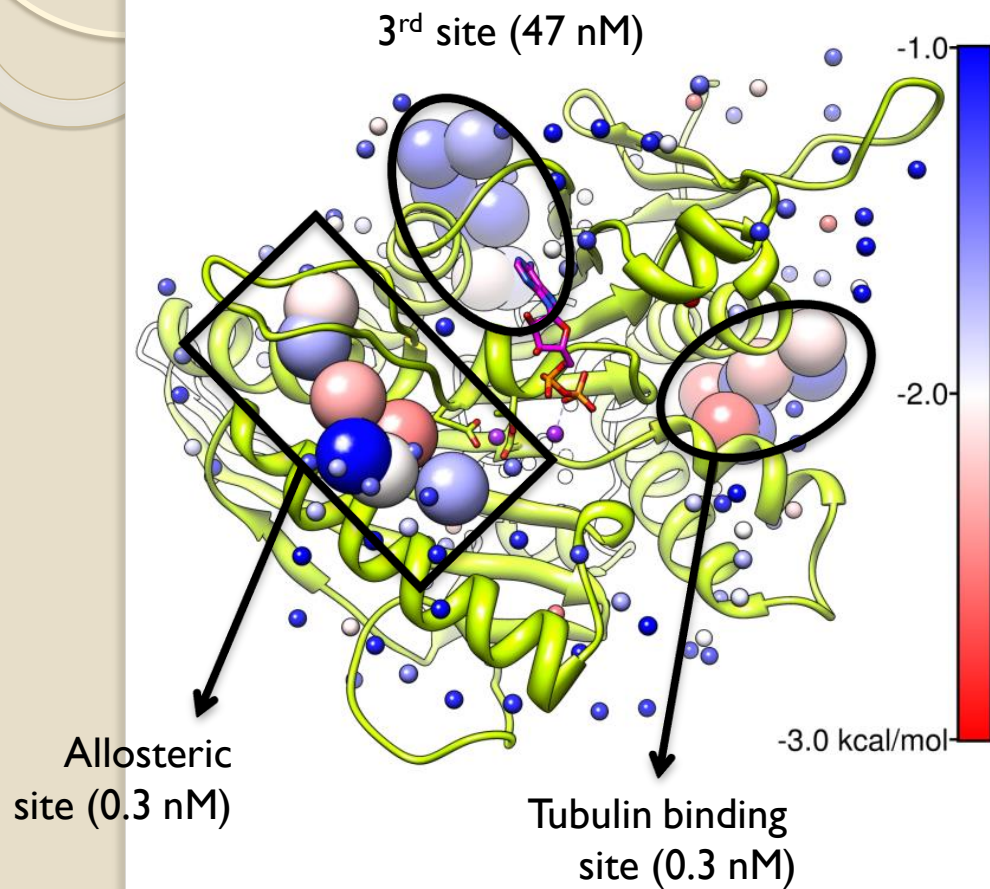


HAC = 32  
MW = 580

# Proteins may have multiple target sites

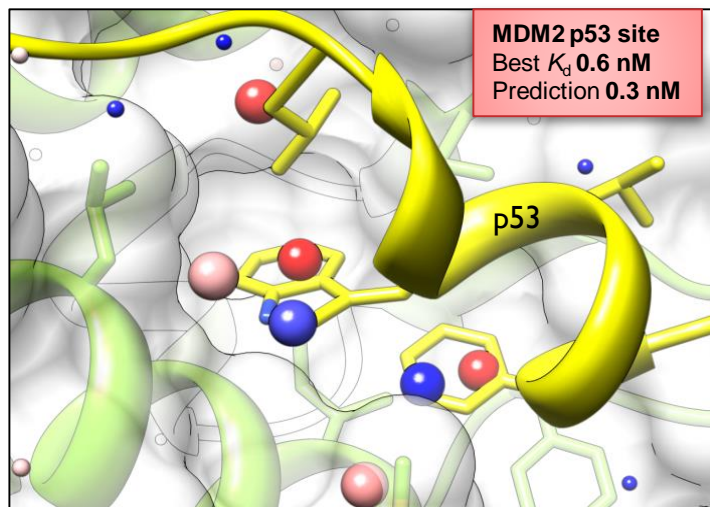


# eg5 Druggable Sites

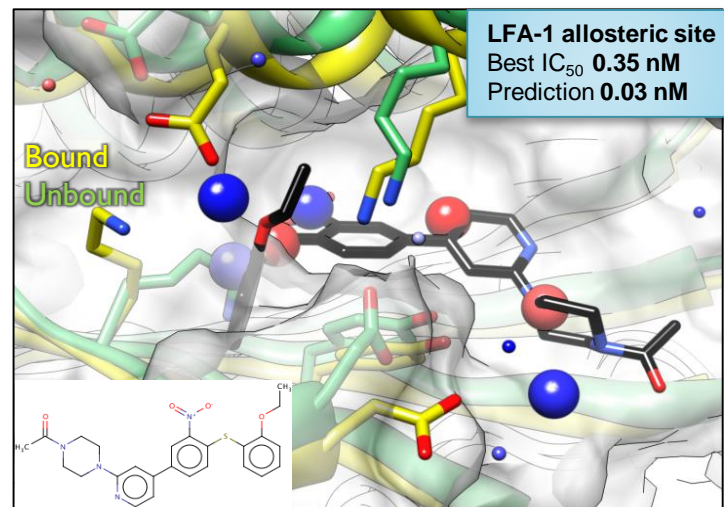


*Bioorg. Med. Chem. Lett.* 2007, 17, 5677-5682

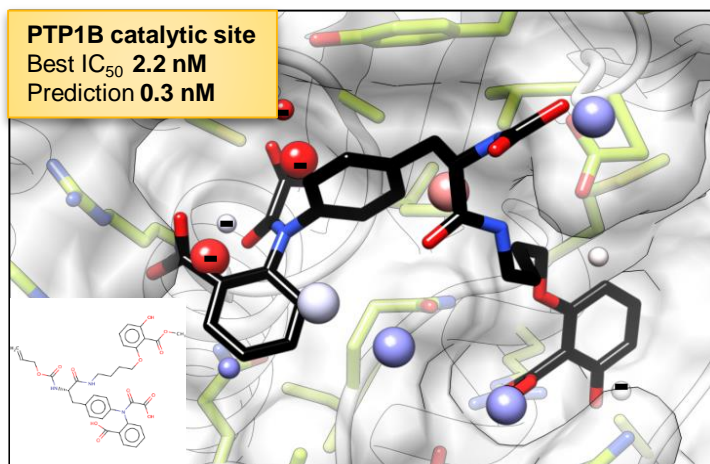
# Assessment of druggable allosteric sites



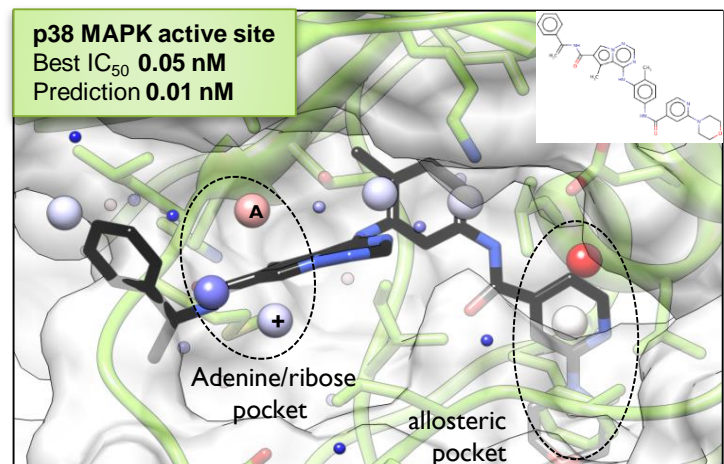
*J Med. Chem.* **2009**, 52, 7970-7973



*Biochemistry* **2004**, 43, 2394-2404



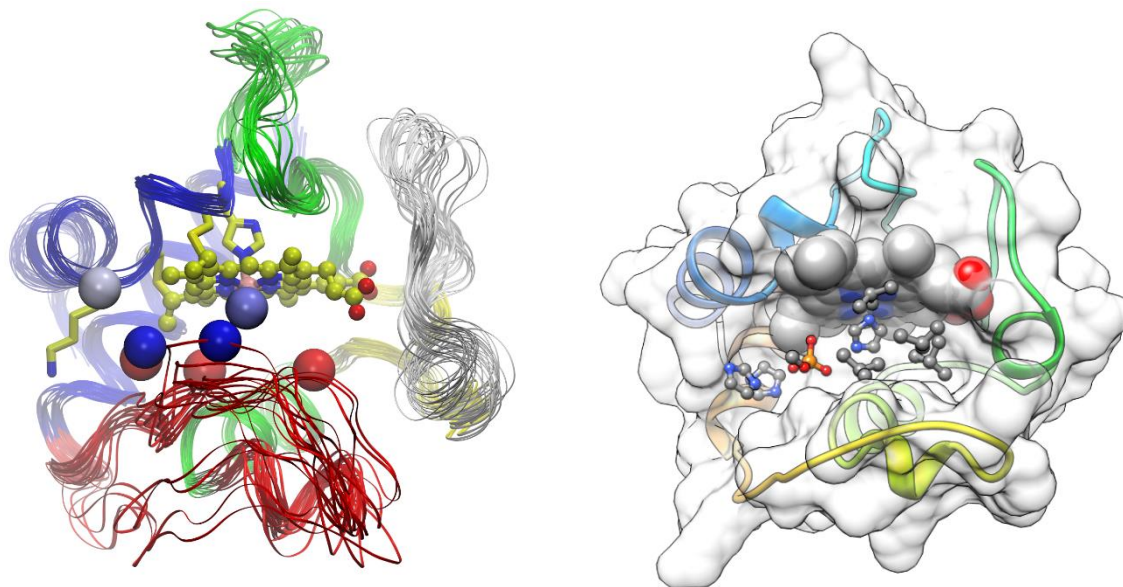
*Bioorg. Med. Chem. Lett.* **2003**, 13, 3947-3950



*J Med. Chem.* **2010**, 53, 2973-2985

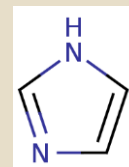
# Discovery of inhibitors of cytochrome c peroxidase activity

druggability simulations for designing a pharmacophore model

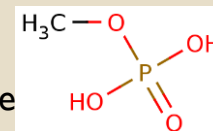


## Probes

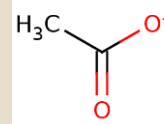
48x  
imidazole



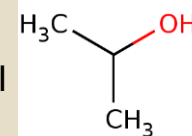
24x  
methyl  
phosphate



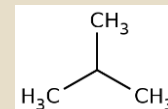
12x  
acetate



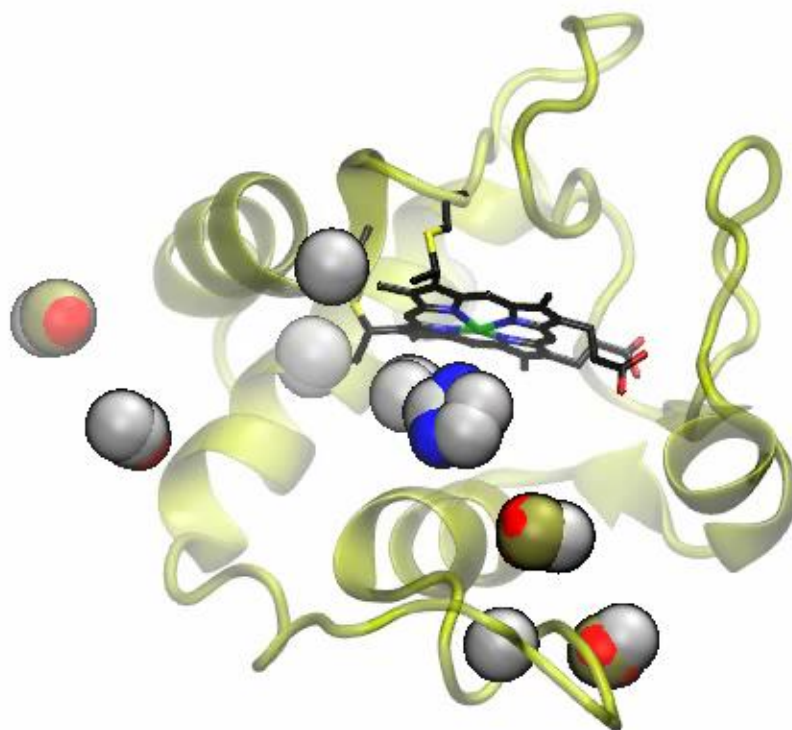
12x  
isopropanol



24x  
isobutane



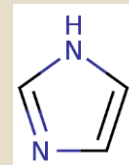
# Discovery of inhibitors of cytochrome c peroxidase activity



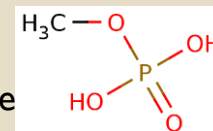
Heme site is the only druggable site with nanomolar achievable affinity

## Probes

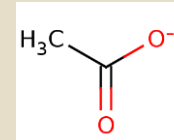
48x  
imidazole



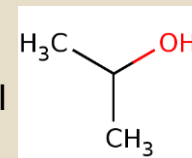
24x  
methyl  
phosphate



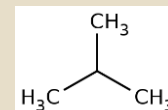
12x  
acetate



12x  
isopropanol

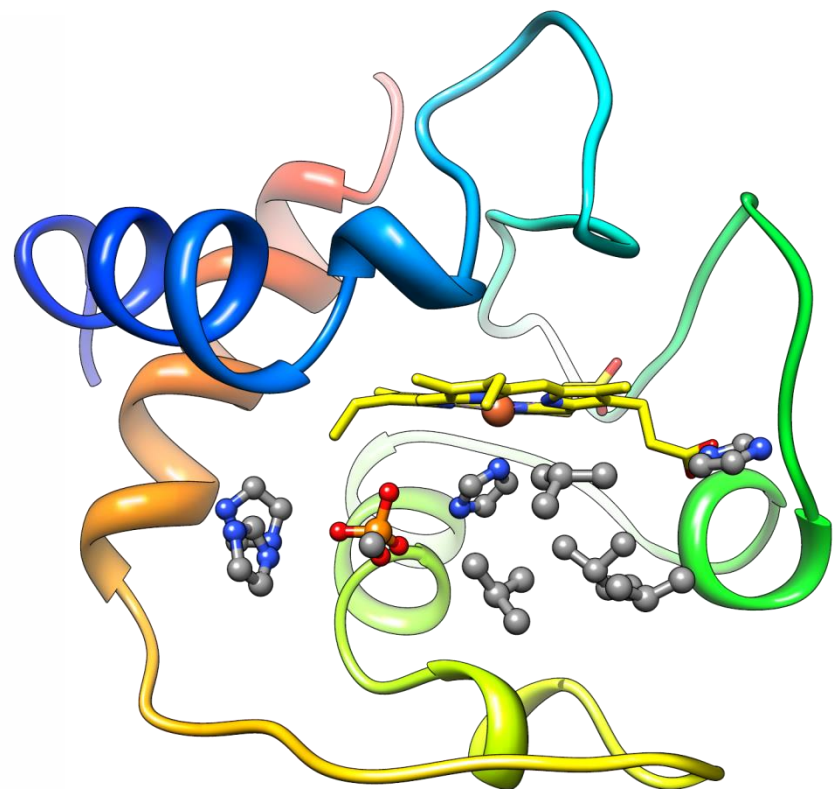
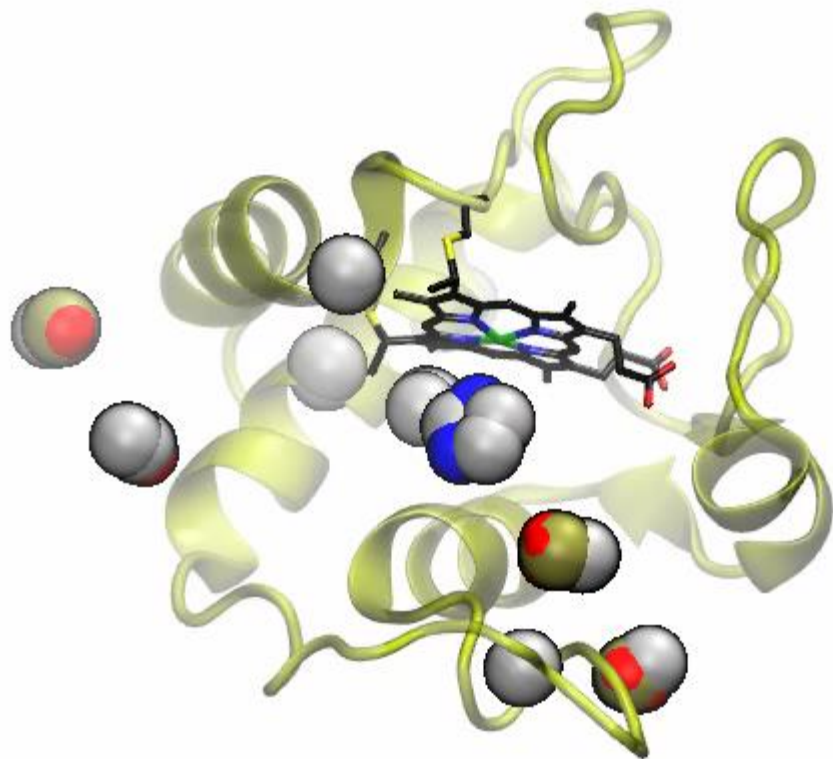


24x  
isobutane



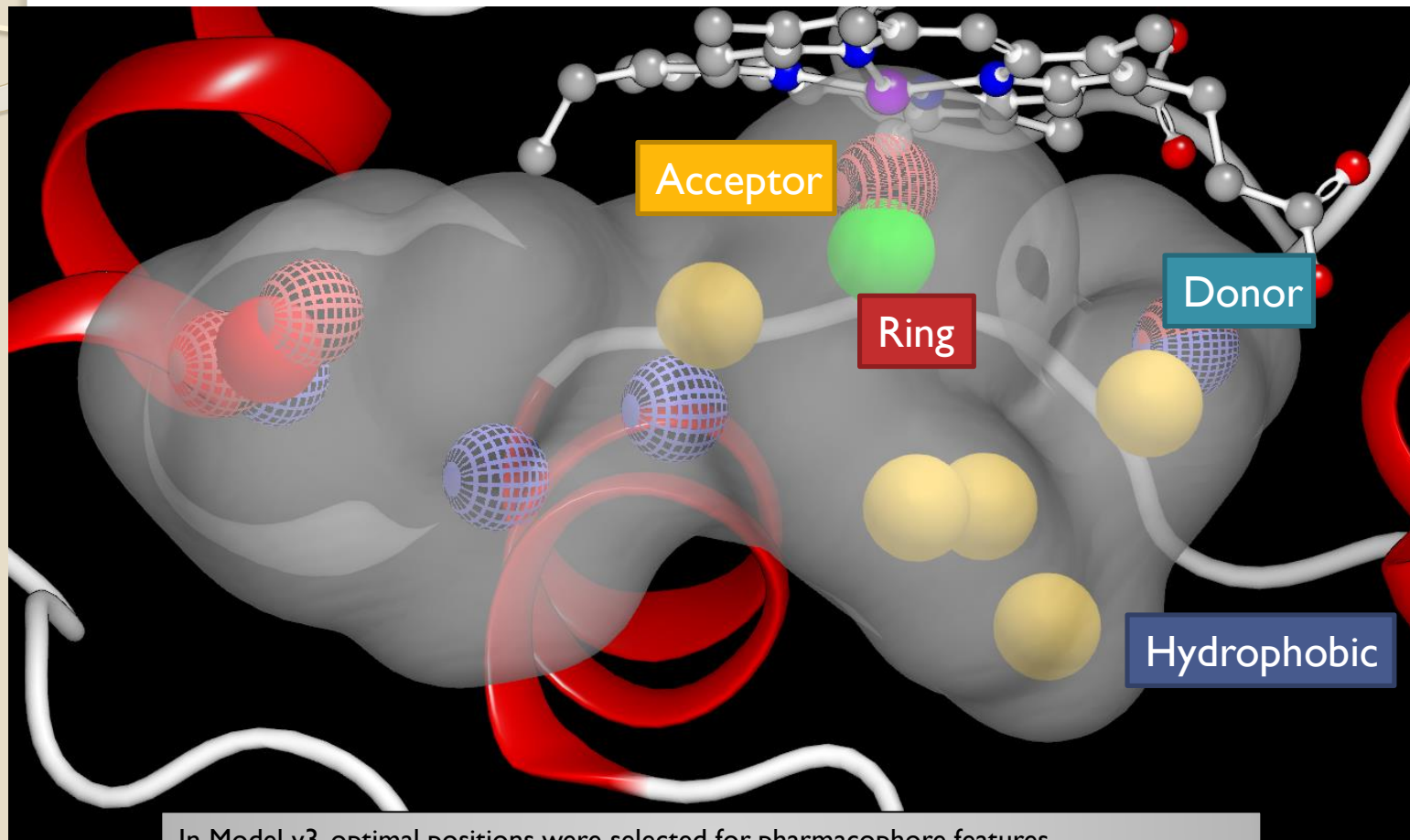


# Probe Simulations



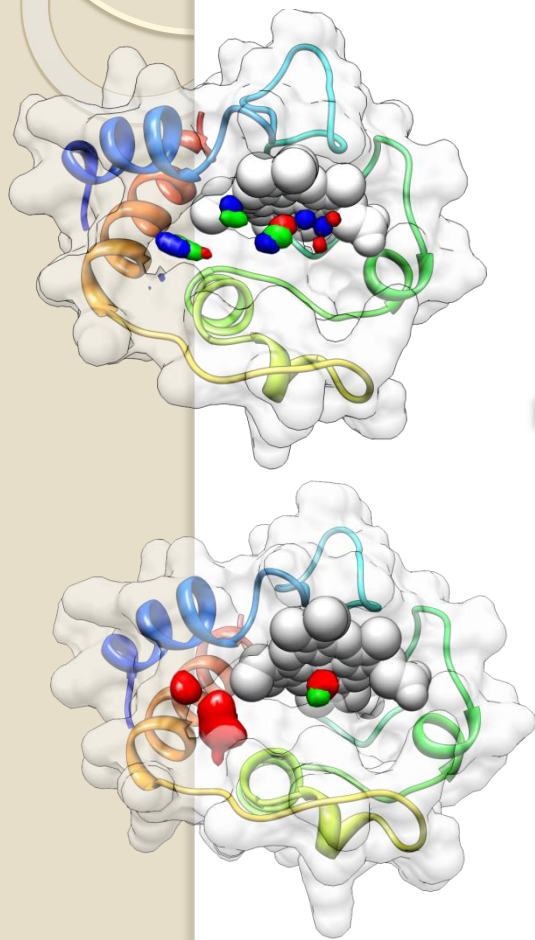
*Snapshots from simulations were used to develop a pharmacophore model*

# Pharmacophore Model

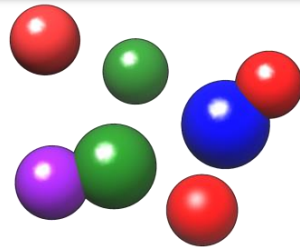


In Model v3, optimal positions were selected for pharmacophore features

# In silico screening



Build a consensus pharmacophore model

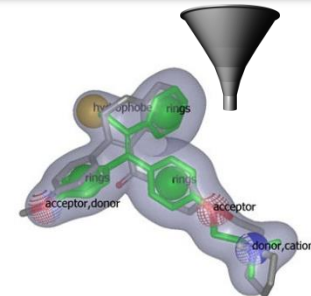


Test ~10-20 compounds



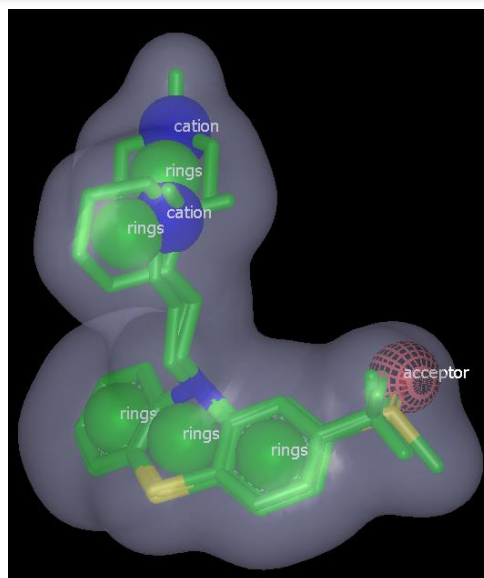
DRUGBANK ZINC

Screen virtual libraries  
~6,000 approved or investigational drugs  
7.5 million purchasable compounds



# Virtual HTS for hit identification

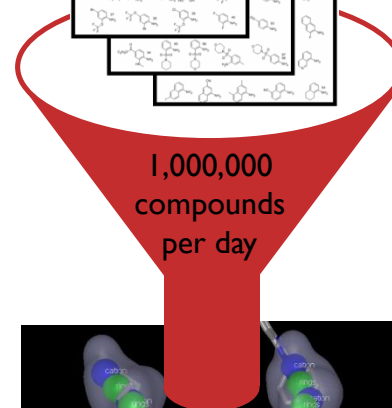
A **pharmacophore model** describes features common to a set of compounds active against a target protein



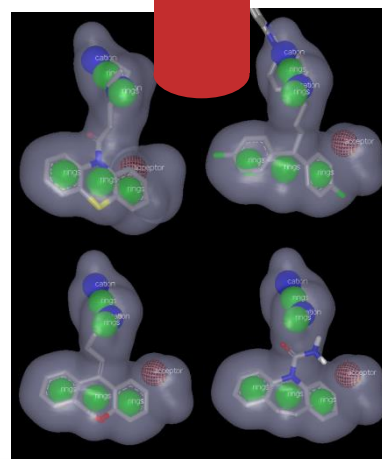
The **virtual HTS pipeline** will allow for identifying *more potent* compounds with similar shapes but diverse chemistry providing us with more choices for chemical synthesis and rational design

**3. Perform virtual high throughput screening** of databases of compounds available for

purchase

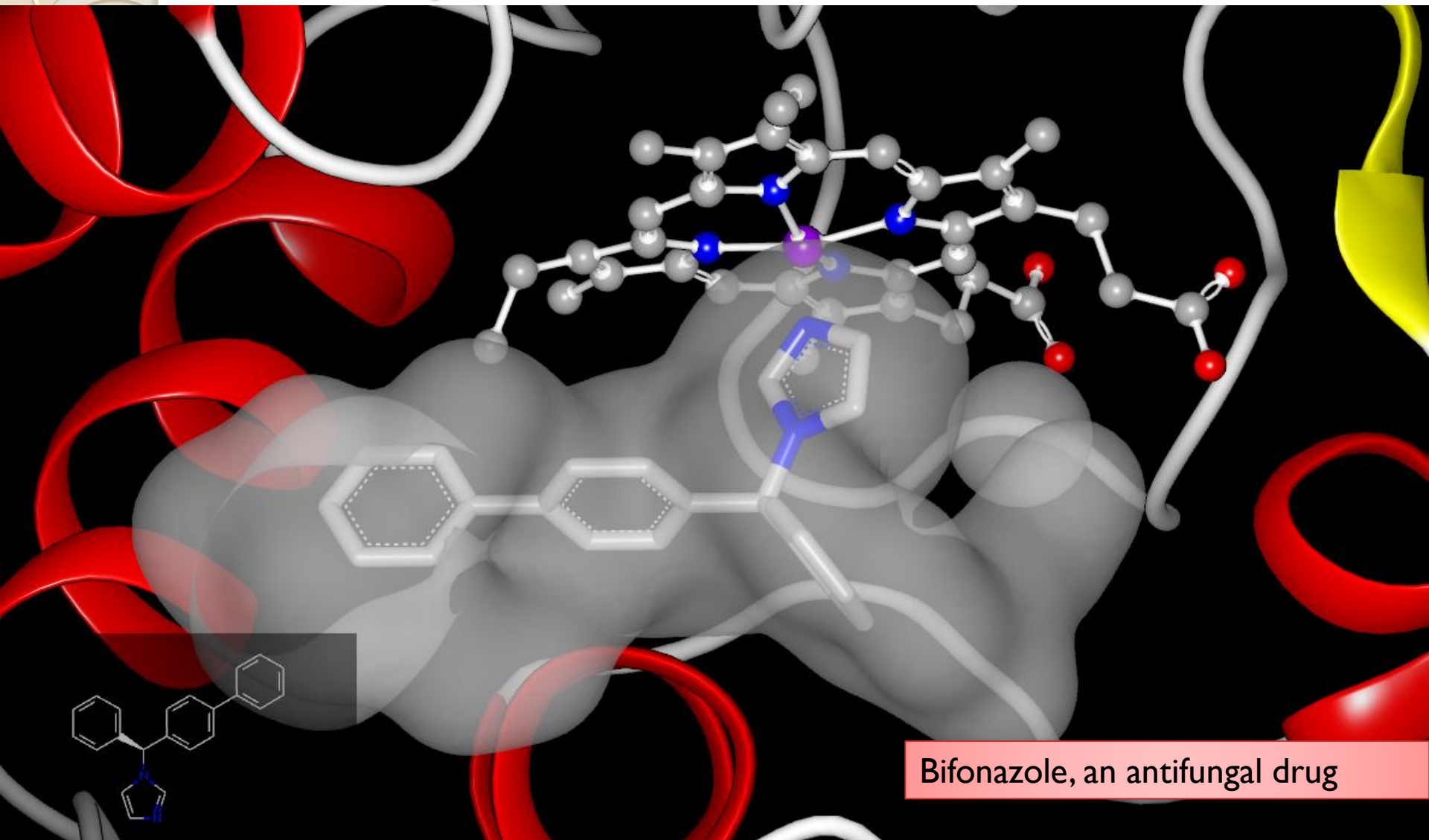


1,000,000  
compounds  
per day



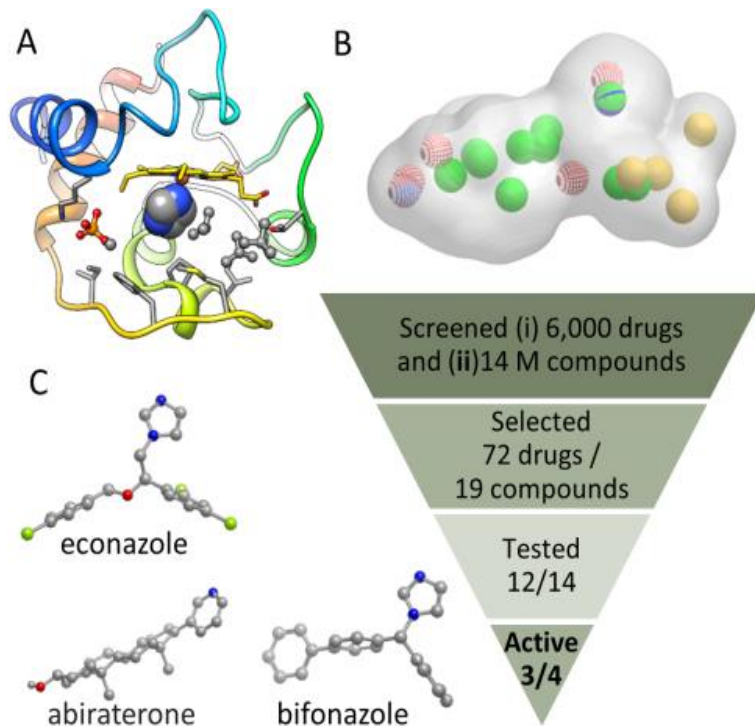
**4. Test virtual hits experimentally** and use results to refine the model

# Example *in silico* hit



Bifonazole, an antifungal drug

# Discovery of inhibitors of cytochrome c peroxidase activity



## Cyt c inhibitor discovery and drug repurposing

A. A snapshot from cyt c druggability simulations

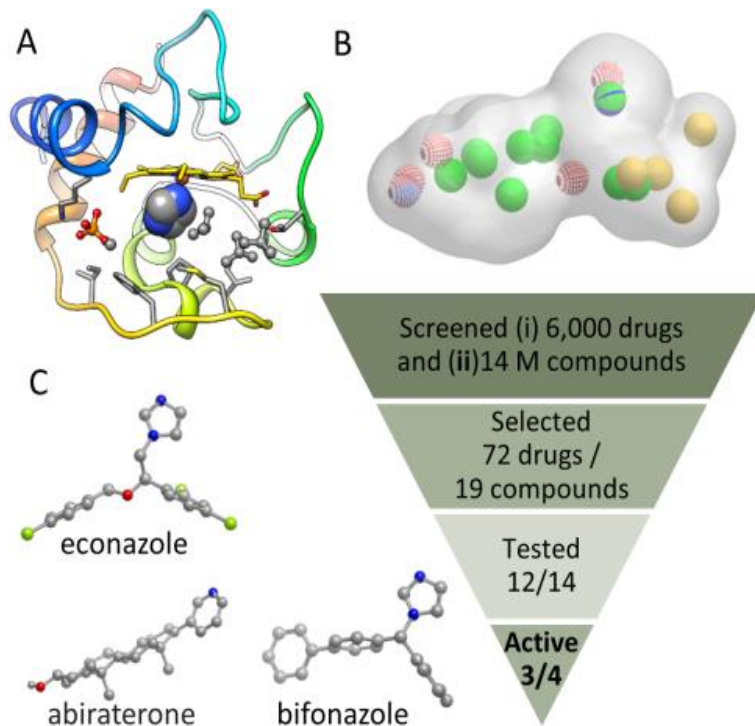
B. Pharmacophore model that was built based on tightly bound molecules observed in druggability simulations.

C. This model was used for virtual screening of 6,000 approved and experimental drugs; 72 repurposable drugs were identified, of which 12 have been tested, and 3 turned out to inhibit *cyt c* peroxidase activity, shown in panel C.

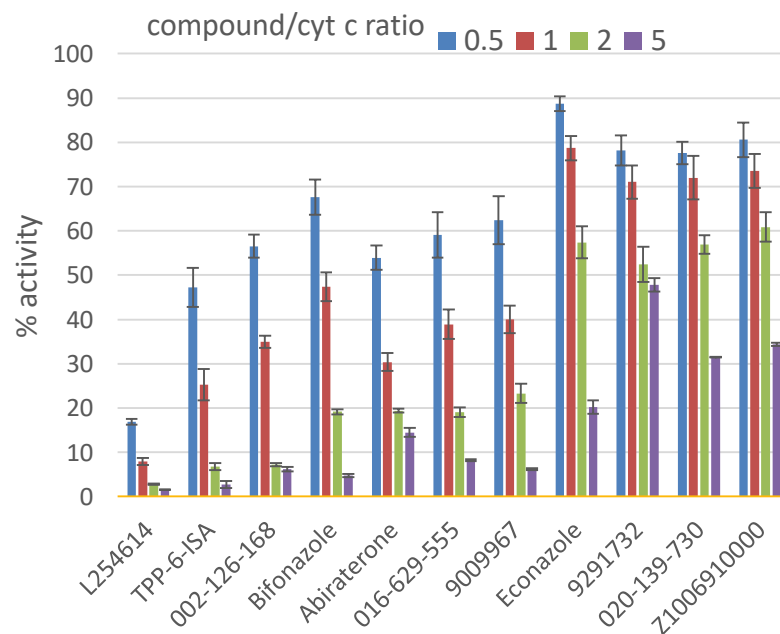
Additionally, 14 M purchasable drug- and lead-like compounds from the ZINC database were screened, 19 compounds were identified, 14 of which tested, and 4 turned out to be novel inhibitors of *cyt c*.

**7 novel inhibitors of peroxidase activity of *cyt c***

# Discovery of inhibitors of cytochrome c peroxidase activity



## Exp validation



Peroxidase reaction probed by fluorescence of oxidation product, for cyt c incubated with CL/DOPC liposomes

# Druggability simulations - summary

## Purpose:

For a first assessment of druggable sites

Identification of allosteric sites that can bind drugs

Assessment of achievable binding affinity

## How ?

Preprocessing: Using probe set either available, or customizable

Prepare input files for NAMD runs (i.e. ensemble of structures with selected composition of probe molecules)

Post-processing: Analyze trajectories generated by NAMD to make inferences on binding sites and affinities, and pharmacophore models

## More:

Screen pharmacophore model, against libraries of small compounds

Provides initial hypotheses, to be validated by experiments

Hits confirmed by experiments can be further evaluated by atomic simulations (including free energy perturbation methods)



# Support from NIGMS, NLM, NIDDK & NIAID

